UR1994_05

1141

TASMANIA DEVELOPMENT AND RESOURCES

Mineral Resources Tasmania
REPORT 1994/05

A study of the nature and origin of gold mineralisation, Mangana–Forester area, northeast Tasmania

by J. Taheri
and
R. S. Bottrill

with contributions by
R. A. Keele
and
G. R. Green

MINERAL RESOURCES TASMANIA PO BOX 56 ROSNY PARK TASMANIA AUSTRALIA

CONTENTS

FIGURES

Abstract

Gold-bearing quartz veins in northeast Tasmania occur in a 90 km long NNW-trending belt between Mangana and Lyndhurst, and are hosted by the metasedimentary Mathinna Beds. The gold mineralisation is of mesothermal type and is typical of many other 'turbidite hosted' gold-lode deposits. Paragenetically, the quartz veins may be divided into three broad categories:

1. Early veins, which include barren fibre veins, and economically significant grey, laminated and/or brecciated veins;
2. Intermediate veins which are white in colour, erratic in sulphide and gold content, and may show comb, buck, breccia and ladder textures; and
3. Late veins, including spider quartz veinlets and narrow veinlets of sulphides or carbonates ± quartz.

Grey quartz veins are economically the most significant and occur in most of the gold prospects.

Hydrothermal wall rock alteration is mainly limited to silicification and carbonate alteration. The latter appears to be related to the gold mineralisation and occurs as small rounded porphyroblasts of Mg-siderite in pelite in close proximity to the gold mines, mainly in the southern part of the field.

Gold grains range from sub micron size to about 1 mm, and occur mainly as:

1. small inclusions in arsenopyrite and quartz;
2. micro-veinlets in coarse, brecciated arsenopyrite, quartz and slate;
3. intergrowths with secondary lead-aluminum arsenates; and
4. intergrowths with goethite.

Compositionally the gold grains are homogeneous and are high in fineness (920 to 990) with the exception of some gold grains from the Linton deposit which have a range of fineness from 654 to 661.

The gold-bearing quartz veins were formed from two distinct types of fluids:

1. H_2O-CO_2 (CH_4)-rich, low salinity fluids with temperatures of around 300°C. These fluids were characterised by high and consistent oxygen isotope values for the early and intermediate quartz veins, ranging from 9.2 to 11.4‰. The data are compatible with a deep-seated metamorphic fluid, probably resulting from devolatisation of metamorphic rocks at depth. However deeply convecting, chemically-modified meteoric fluids may also have played an important role. These fluids were responsible for the formation of vast majority of the gold-lode deposits;
2. Rarer CO_2-poor fluids of possibly lower formation temperatures with lower oxygen values of 6.9 to 9.0‰, similar to the isotopic composition of fluids responsible for the greisenisation of granites. These quartz veins exhibit different mineralogy and contain wolframite and tourmaline, and are anomalous in Sn and W. The results are indicative of the involvement of a granitic intrusion in the formation of these gold-lode deposits (e.g. Gorge Creek Tungsten prospect).

Reduction in activity of sulphur, together with a decrease in temperature caused by boiling of fluids, appear to have been an effective mechanism in precipitating the gold in the early-formed quartz veins. Wallrock-fluid interaction appears to have played a less important role in the formation of gold deposits along the gold belt.

Sn and W and oxygen isotope analyses, together with fluid inclusion studies, are effective techniques in differentiating the quartz veins of metamorphic origin from those formed as a result of granite intrusion.

INTRODUCTION

Gold-bearing quartz veins occur within a NNW-trending belt, about 1 km wide and approximately 90 km long, extending from Mangana in the south through Tower Hill, Mathinna, Dans Rivulet, Alberton, Warrentinna and Forester to Lyndhurst on the north coast (fig. 1). This investigation covers the area between the Mangana and the Forester goldfields.

Gold mineralisation in northeast Tasmania has been known for more than 140 years and most of the present prospects were discovered by 1900. Gold prospectors in the past discovered some gold mines of very high economic significance such as the Golden Gate mine at Mathinna, where over seven tonnes of gold was recovered between 1881 and 1932. Over 80% of this gold was produced from about 284 350 tonnes of ore between 1881 and 1912. Most of the mines were abandoned before any organised mining development, mainly because of lack of sufficient capital, proper mining development, and insufficient geological knowledge.

To date, after some 140 years, no multi-disciplinary mineral exploration programmes have been carried out within the goldfields; very few deposits have been drilled and most have not been systematically sampled or mapped. There is no geological evidence to suggest that other quartz veins of similar size, continuity and gold content to the Golden Gate mine, once the most significant gold mine in Tasmania, do not exist within the gold belt.

It should also be mentioned that no detailed ore genesis investigation has been undertaken along the gold belt, and recent discussions of the possible structural controls on gold-bearing quartz veins in the last three decades are limited to Threader (1967), Findlay (*in* Taheri, 1992) and Keele (1994).

The aims of this study are to:

1. Investigate the possible origins of the ore-forming fluids (i.e. metamorphic vs granitic), as this may have significant impact on any exploration activities within the area.

2. Identify different quartz vein types and to differentiate the auriferous and barren quartz veins through fluid inclusion, stable isotope, petrographical and geochemical studies.

3. Investigate whether any geochemical or stable isotope techniques can be used in differentiating the possible different styles of mineralisation.

The results obtained from this study, together with those obtained by Keele (1994), provide a better and modern understanding of the structure and genesis of the gold-bearing quartz veins along the gold belt.

HISTORY AND PRODUCTION

Mangana Goldfield

The Mangana goldfield was the site of the first discovery of payable gold in Tasmania. The goldfield was discovered by James Grant of Tullochgorum in February 1852, on Richardsons Creek near Mangana ("about 150 metres below the present bridge": Twelvetrees, 1907). Most production occurred between 1852 and 1910, but has been sporadic. The first lode gold mining in the area commenced at the Sovereign mine in April 1859 (Twelvetrees, 1907; Blake, 1939). Some alluvial mining resumed at Majors Gully into recent years.

Table 1

Gold production, Mangana goldfield (adapted from McOnie, 1983)

Mine	Gold production (kg)	Tonnes ore	Average grade (g/t)
Abbotsford Creek	0.22	1525	0.14
Alpine	19.19	27.5	?
Buckland	35.88	1421	25.25
Cardinal	4.91	240	20.48
Fingal	9.88	9.10	
Golden Entrance	91.41	718	127.31
Golden Gully	-	0.8	?
Great Fingal	1.00	5	199.06
Mangana	24.60	3106	7.92
Miami	19.91	795	25.04
Pinchers	0.31	10	31.10
Richardsons Creek	-	40.6	-
Tower Hill Freehold	-	61.2	?
Union Jack	0.31	20	15.55
West Miami	0.23	27	8.41
Miscellaneous alluvials	~150		
Total	207.85	8057.6	25.80

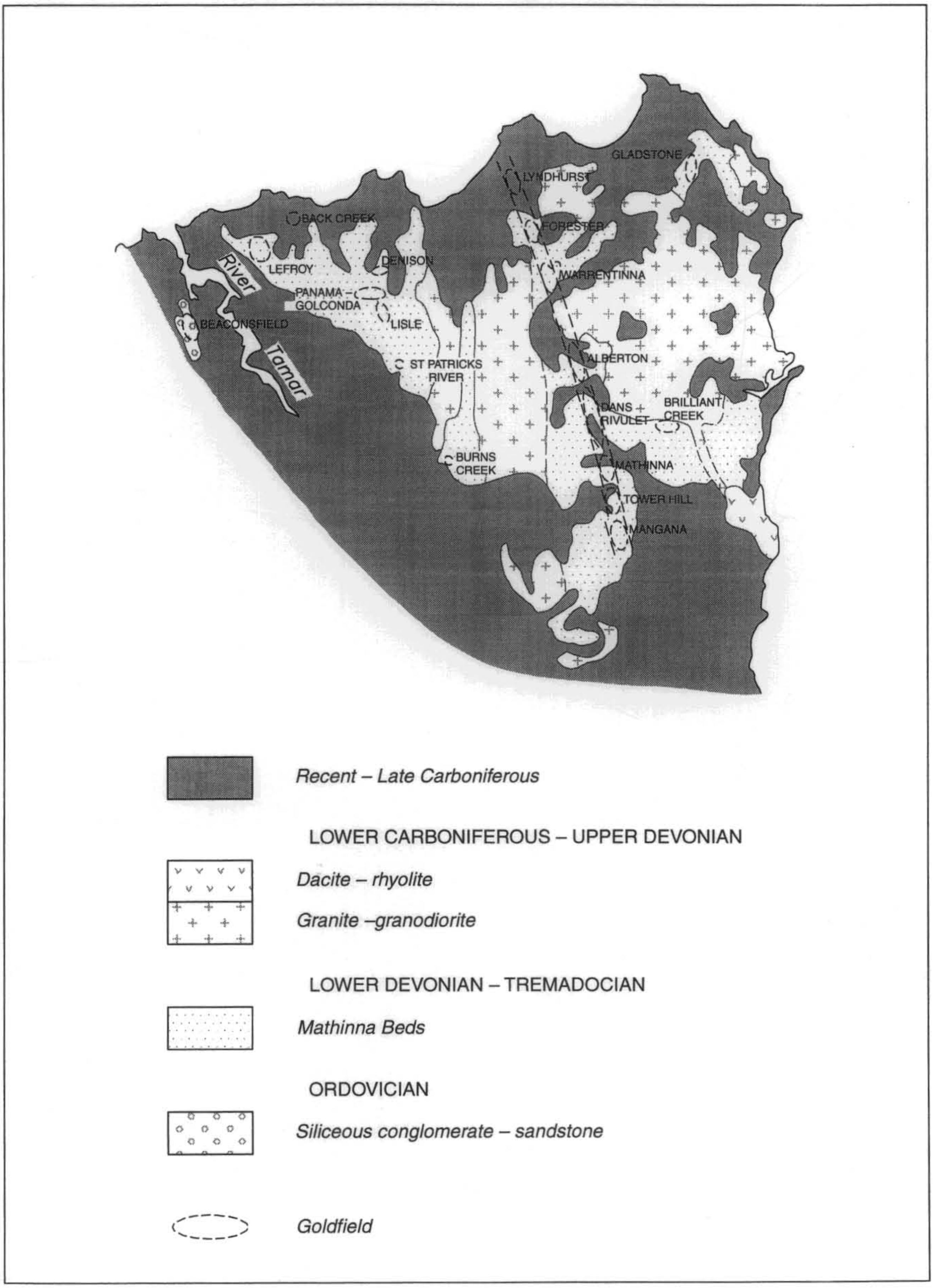

Figure 1

Location of goldfields, northeast Tasmania

5 cm

The total recorded production from the lode deposits in the area is 208 kg (Table 1) but, as early records are poor, the actual production could have been much greater. Between 5,000 and 15,000 ounces (about 160–470 kg) of gold was also produced from alluvial deposits (Twelvetrees, 1907). Some of this alluvial gold was apparently traced to conglomerates in the Parmeener Supergroup, but no production from palaeoplacers in these rocks has been recorded (Twelvetrees, 1907). A large proportion of the gold was probably taken directly to the mint in Victoria by the miners. The largest mine in the area was the Golden Entrance, which had a recorded production of 90 kg of gold (2939 oz) at an average grade of 125.3 g/t. In comparison, the Golden Gate mine in the contiguous Mathinna goldfield, approximately 10 km to the north of Mangana, had a recorded production of 7.896 t (253,865 oz) at an average grade of 26 g/t (Noldart and Threader, 1965).

Mathinna Goldfield

The Mathinna Goldfield was one of the earliest goldfields discovered in northeast Tasmania. Gold was probably discovered in the Mathinna area a few years after the first discovery of gold near Fingal in 1852 (Finucane, 1935). By 1892 most of the presently known gold prospects within the area had been discovered and worked downward from the surface to depths of less than 30 m, with the exception of a few mines in which the lodes were worked to greater depths (e.g. New Golden Gate mine). Most of the mines were abandoned before any organised development. This was mainly because of:

(a) narrowing or lowering of grades of gold-bearing quartz veins laterally or vertically;

(b) lack of sufficient capital for proper mining development; and

(c) displacement and disturbance of quartz veins by faults and shears (Montgomery, 1892; Twelvetrees, 1907; Finucane, 1935).

Consequently the goldfields were labelled as being "patchy and unreliable" (Montgomery, 1892).

Extensive but superficial attention has also been paid to the Dans Rivulet goldfield. According to Hughes (1947), within the goldfield "every square mile has been vigorously prospected, thousands of shallow trenches dug, many adits driven and shallow shafts sunk, but seldom have the depths exceeded a hundred feet or so". It appears that the exploration took place at a very low level and small scale, with consequent low returns. This was blamed on the lack of profitable gold shoots, and the goldfield lost its attraction to exploration and mining companies.

Recent exploration activities including those of the Electrolytic Zinc Co. of Aust. (EL 2/59, 1959–62); Texins (EL 6/68, 1968–74); ACA Howe Aust. Pty Ltd (EL 31/76, 1977–86); Tasminex (EL 17/78, 1978–82); Pegasus Gold Aust. (EL 55/83, 1983–90); Goldfields Exploration Pty Ltd (EL 17/86, 1986–88); Australian Anglo American Ltd (EL 22/80, 1980–82); and Cuttack Mining and Exploration P/L (EL 53/89, 1990–91). These companies also did not apply any novel techniques to locate undiscovered gold lodes or extensions to the known lodes.

Consequently, geologist's recommendations regarding diamond-drilling programmes could not be justified by the companies. This was mainly because of the high cost of drilling and the perception of only small gold lodes being present within the area. More recent exploration programmes have mainly been focused on the mine tailings and some alluvial gold deposits.

To date, about 120 years after initial development, no systematic exploration programme has been carried out within the goldfields and there is no geological evidence to suggest that other profitable and relatively large-scale vein-type gold deposits, similar to the New Golden Gate mine, might not exist in the area.

The Mathinna goldfield had the highest officially recorded gold production in the area of 8.265 t (288,986 oz) between 1880 and 1932 (Montgomery, 1892; Twelvetrees, 1907, 1914; Finucane, 1935). From this total, 7.197 t (253,865 oz) was produced from the Golden Gate mine and 0.312 t (10,997 oz) from the Tasmanian Consols mine (Tables 2, 3). However the true production may have been higher, as Twelvetrees (1914) reported from "official returns" a total gold production of 8.805 to 9.072 t (300,000–320,000 oz) from the Mathinna goldfield up to 1914. The Dans Rivulet goldfield produced at least 140 kg (4938 oz) of gold in the period 1888 to 1906 (Table 3) (Hughes, 1947; Twelvetrees, 1907). The only recorded gold production from Tower Hill was 0.12 kg obtained from the Sunbeam mine (Table 2).

There are no records of alluvial gold production from the Mathinna, Dans Rivulet and Tower Hill goldfields, probably because (according to local residents) the fields were mostly worked by the Chinese who did not keep any gold production records. However the potential for the occurrence of significant alluvial deposits in Black Horse Gully, Long Gully Creek, and in the Dans Rivulet and South Esk River valleys was recognised long before 1870. According to Twelvetrees (1907) small nuggets of up to 6 to 8 grams were common in the early days of mining, and a piece weighing 120 grams was also found in the Black Horse Gully and Long Gully Creek area. A drilling programme, consisting of 87 holes drilled at about 20 m intervals along lines 160 to 200 m apart, was carried out at the mouth of Black Horse Gully before 1906 (Twelvetrees, 1907). The average yield was about one gram of gold per cubic metre over an average depth of two metres.

Later work on the alluvial deposits in Black Horse Gully, Long Gully Creek, and north and east of the South Esk River (e.g. Turner, 1972) indicated that the distribution of gold grains was erratic and below the grades mentioned by Twelvetrees (1907). It should be emphasised that the majority of past programmes were not carried out systematically, and estimated reserves may not reflect the true values. Some small alluvial mines are presently operating in the areas near O'Briens Creek and in Black Horse Gully.

Table 2

Gold production, Mathinna and Tower Hill goldfields (Finucane, 1935)

Deposit	Ore* (tonne)	Gold* (kg)
Welcome Stranger	-	-
Enterprise	10	0.93
New Golden Gate mine	304 158	7 197.10
Tasmanian Consols (North Golden Gate)	34 236	311.76
South Golden Gate	-	-
Caledonian	-	-
New Eldorado (prior to 1886)	508	?
	579	26.22
Horseshoe	89	1.43
Gladstone	71	1.12
Miner's Dream	208	12.29
Old Boys	242	2.14
Volunteer Mine	~9 000	72.79
Volunteer Consolidated	1 788	35.79
Yellow Boy	213	2.41
Chester and Murray	2.5	0.03
	?	2.55
City of Hobart	?	596
Pride of Hills	91	?
	15	0.23
Scott and Pickett	93	1.07?
Mountaineer	-	-
Jubilee	56	1.67
Sunbeam (Tower Hill Goldfield)	12	0.12
Total	8 265.73	

* Recorded or quoted values

Table 3

Gold production, New Golden Gate mine (Finucane, 1935)

Period	Ore (quartz) (tonne)	Gold (kg)
to 1881	406	3.923
1881–1912	284 351	6 650.992
1913	?	31.612
1914	1 565	29.23
1915	2 171	78.643
1916	?	43.177
1917	551	9.157
	1 016 (tailings)	28.350
1918	1 298	28.520
1919	1 405	40.881
	7 (pyrite)	2.296
1920	985	17.792
1921	?	15.829
1922	1 439	22.748
1923	2 139	26.564
	Other sources	8.420
1924	?	44.550
1925	?	15.125
1926	1 609	41.986
1927	?	49.882
1928	265	6.070
	2 956 (tailings)	8.300
1929	213	
	1 172 (tailings)	10.892
1930	260	4.488
	333 (sands)	1.604
1931	260	4.488
1932	?	1.050
Total	7 197.10 (253 865.10 oz)	

Alberton Goldfield

Auriferous quartz veins were first discovered in the Alberton area prior to 1883 (Thureau, 1883). Over 100 gold-bearing lodes were worked intermittently between 1883 and 1939, although most prospecting and mining took place before 1900. By 1904 only a few mines, namely the Long Struggle, New Mercury, McCaul Brothers and the Ringarooma, were still operating (Twelvetrees, 1904).

Until the late 1960s geological information was restricted to descriptions by Government geologists including Thureau (1883, 1884), Twelvetrees (1904), Hills (1923), Reid (1925), Nye (1933), Scott (1933), Blake (1938), Hughes (1952) and Threader (1967). These early reports described the mineralisation and mining and milling history of some deposits.

The Alberton goldfield, like most other gold fields in northeast Tasmania, has not been systematically studied or explored. Most geologists have realised the under-developed state of the mines and some recommended more systematic exploration programmes and proper mining development for the goldfield. However the companies either lacked sufficient development capital or were not convinced that the discovered lodes deserved any more systematic investigation.

At one stage the area was expected to become the richest goldfield in Tasmania (Hughes, 1952). However most of the lodes were worked over a short strike length to shallow depths of commonly less than 60 m, with the deepest being the Ringarooma United mine which was mined to a depth of about 119 metres.

The Alberton goldfield is characterised by the highest density of relatively gold-rich lodes among the northeast goldfields, but factors such as the erratic distribution and gold content of quartz veins, and the under-capitalised nature

TABLE 4

Gold Production, Alberton Goldfield

Deposit	Ore (t)	Gold (g/t)	Gold (kg*)
Alberton Quartz Mine (No. 1 and No. 2)	173	28	4.82
	47	12	0.55
Crown Prince	102	27	2.70
	10	28	0.28
	51	"Low"	-
Forest King (Jan's)	30	71	2.13
Bright Star	"First stone"	>29	?
	"Later Crushings" (Twelvetrees, 1900)	~20	?
Brown's	10	71	0.71
Esk	4	15	0.060
Telegraph (Duke's)	6	7	0.04
Caxton	"Several Crushings" Twelvetrees (1904)	24	?
	30	28	0.84
	102	24	2.40
Tiger	102	28	2.8
	-	10	?
Pennefathers	14	30	0.42
	30	20	0.60
	51	?	-
McCaul	30	20	0.60
South Ringarooma	54	42	2.23
	19	66	1.25
	9	55	0.50
	12	32	0.39
	47	13	0.6
	47	12	0.55
Mt Victoria	?	20–60	145.76
New River	-	~30	130.83
Ragged Youth	?	20–50	7.34
New Mercury	94	10	9.20
	100	22	2.16
	109	10	1.07
Premier	-	~10	-
Ringarooma Gold Mining Co.	?	~30	255
Reform	17	1.4	0.24
	8	45	0.36
Mallunnah	38	20	0.74
Long Struggle	"Trial Crushing" (Twelvetrees, 1904)	95	-
		35	19.11
	59	50	3.00
Short Struggle	"Small Crushings" (Twelvetrees, 1904)	57	?
Frog	10	93	0.93
Boundary	5	2	0.11
New Mercury	-	-	46

* Recorded, quoted or estimated values.
References: Hills, 1923; Twelvetrees, 1900, 1904; McOnie, 1983.

of the companies, prevented the evaluation of the full potential of the goldfield.

An accurate total of gold production for the Alberton goldfield is not known. However according to Hills (1923) £60,000 worth of gold, equivalent to approximately 425 kg of gold, was won from the field. Of this total about 255 kg of gold was obtained from the Ringarooma United mine.

The first, and possibly the richest ore, was reported by Thureau (1883) in which a 960 g sample yielded 21 g of gold. Gold values up to 120 g/t were also recorded by Twelvetrees (1904).

A summary of gold production for different prospects is shown in Table 4. Several exploration companies, including the Stanton Engineering Company (EL 6/76), Amdex Mining Ltd (EL 7/80), Gold Fields Exploration Pty Ltd (EL 26/85 and 17/86), Oceania Pty Ltd (EL 23/82) and Billiton Australia have been active in the area, although the exploration programmes were mainly limited to literature review and some non-systematic rock-chip and steam-sediment sampling.

Mt Horror Goldfield

Gold was first discovered at Warrentinna in the 1880s and most production occurred between 1880 and 1920. The first gold mining in the Forester area was much later, about 1922.

The total recorded production from lode deposits in the area is only 105.16 kg (Table 5) but, as early records are poor, the actual production could have been much greater. The largest mine in the area was the Golden Mara, which had a recorded production of 104.4 kg of gold at an average grade of 29 g/t. In comparison, the Golden Gate mine, in the Mathinna goldfield to the south, had a recorded production of 7.896 t (253,865 oz) at an average grade of 26 g/t (Noldart and Threader, 1965).

Table 5

Production and grades of gold mines in the Mt Horror area

Mine	Gold production (kg)	Ore mined (tonnes)	Av. grade (g/t)
Dawn of Peace	0.19	6	31
Golden Mara	104.41	3560	29
Imperial	0.47	20	23
Jordans	0.09		
Total	105.16		

REGIONAL GEOLOGY

The geology of northeast Tasmania has recently been described by Bottrill (1992), Taheri (1992), McClenaghan (1985), Williams *et al.* (1989), Green (1990), Powell and Baillie (1992), and Powell *et al.* (1993), from which most of this summary has been taken.

The focus of this report is a 70 km long section of the NNW-trending belt gold belt, which extends northwards from Mangana, through Mathinna and Alberton to Forester (fig. 1). The total belt is 90 km long from Fingal in the south to Lyndhurst on the north coast, and occurs within the Mathinna Group, an apparently conformable turbidite sequence, ranging in age from Early Ordovician, or older, to Early Devonian. The Mathinna Group rocks consist of sandstone (quartzose sublitharenite to feldspathic litharenite), and mudstone (Powell *et al.*, 1993), the latter locally metamorphosed to slate and schist. There is no firm control on the age of the Mathinna Group in the area of this report, the nearest fossil locality being in the Golden Ridge area, 15 km NE of Mathinna, where graptolites of Ludlovian (middle Late Silurian) age have recently been found (Rickards *et al.*, 1993).

The rocks are folded about NNW-trending axes subparallel to the trend of the basin of deposition (Powell *et al.*, 1993). A strong NW-trending cleavage is developed. Syn-tectonic extensional fractures, now filled with quartz, are developed in fold limbs and hinges. The bulk of the deformation probably occurred before granitoid emplacement between 395 ± 1.5 Ma and 348 ± 10 Ma as the granitoids crosscut folds in the intruded rocks. At St Marys, most regional folding preceded the eruption of the 388 ± 1 million year old St Marys Porphyrite, a thick welded ignimbrite related to a nearby granodiorite dyke. The porphyry occupies a cauldron structure and unconformably overlies the Mathinna Group, but later folding affected both the country rock and porphyry, probably while the latter was still cooling (Turner *et al.*, 1986). Hornfelsing is common in narrow aureoles adjacent to Devonian granite intrusive rocks (McClenaghan, 1985), and sub-vertical elongation of associated metamorphic spots in slate provides further evidence that deformation continued after granitoid intrusion, as do locally developed tectonic foliations in some granitoid bodies (Williams *et al.*, 1989). Powell and Baillie (1992) have suggested that a major phase of SW-directed thrusting in the Beaconsfield–Lefroy area followed the major folding episode. Goscombe and Findlay (1989) have demonstrated a late-stage event of regional mega-kinking related to a N-S directed shortening.

The granitoids range in composition from granodiorite to granite and include both I- and S- types (McClenaghan, 1985; McClenaghan *in* Williams *et al.*, 1989). The last phase of plutonism produced highly fractionated granites containing fluorite, topaz and apatite and was associated with tin and tungsten mineralisation.

The Mathinna Group and granitoids are overlain unconformably by flat-lying Late Carboniferous to Permian terrestrial and glaciomarine sedimentary rocks, which are succeeded by Triassic fluviatile sandstone-dominated sequences with minor basalt flows (Turner and Calver, 1987). The upper part of the Triassic sequence is predominantly lithic arenite, mudstone and shale, which contains Tasmania's major coal deposits. Sheets and dykes of Jurassic dolerite intrude these sequences. Tertiary basalt occurs as isolated to extensive basaltic flows in some areas, such as around Alberton and the New River, and exhibits interfingering relationships with mainly fluviatile sediments, some of which have been mined extensively for alluvial tin and gold. Pleistocene to Recent sedimentary deposits fill parts of the major river valleys.

The origin of the gold deposits has been a subject of some debate, partly because very little modern work has been devoted to the subject. The possible structural controls on the distribution of the lodes have been discussed by Hills (1923), Blake (1933), Hughes (1952), Threader (1967), and more recently by Findlay (1993) and Keele (1994). The auriferous quartz veins occur in a NNW-trending belt about one to two kilometres wide characterised by tight folding, extensive shearing, strongly developed cleavage in slate, and abundant quartz veining. Powell (1991) has suggested that the gold mineralisation in the Mathinna Group at Beaconsfield and Lefroy is related to the episode of SW-directed thrusting, but there is little evidence for this phase of deformation in the Mangana–Lyndhurst gold belt. In contrast, Klominsky and Groves (1970) suggested that the gold mineralisation might be related to granodiorite emplacement, and Leaman and Richardson (1992), from the modelling of gravity data, have indicated that some of the deposits might overlie local protruberances in the top of granodiorite intrusives. The Lisle–Golconda area, 40 km west of the gold belt, contains a number of alluvial goldfields which spatially overlie cupolas of weathered granodiorite (Roach, 1992). However no convincing spatial or genetic relationship between gold deposits and granodiorite has been demonstrated generally and for the gold belt in particular.

PARAGENESIS OF QUARTZ VEINS (with a contribution by R. A. Keele)

The overprinting of quartz veins is relatively common within the goldfields, and paragenetically at least three broad generations of quartz ± carbonate ± sulphide veins can be defined:

(1) Early veins include barren fibre veins and the economically important, grey, laminated and brecciated veins. Silicified wallrocks units probably accompanied this stage.

(2) Intermediate veins are white in colour and display buck, comb, breccia and ladder textures. However the paragenesis of the ladder veins is not well established.

(3) Late veins include spider quartz veinlets and narrow veinlets of sulphides or carbonates ± quartz. In addition, white quartz is rarely brecciated and infilled by grey quartz (Golden Gate, Mangana Gold Reef). It is not certain whether this infilling grey quartz is of the early generation (establishing one generation of white quartz as being very early), or is a later phase.

It must be emphasised, however, that detailed relationships are complex and ambiguous, and up to five vein generations have been distinguished in one small sample (e.g. Mt Victoria, sample No. C103855B).

Illustrations of various vein types are given in Keele (1994).

Fibre veins

These veins are characterised by an aggregate of parallel quartz fibres at a high angle to the vein wall, and evidence of multiple growth increments without euhedral terminations. This has been interpreted as a product of crack-seal incremental growth (Cox and Etheridge, 1983; Dowling and Morrison, 1989).

Some quartz veins in the lode environment may have a fibrous texture (Keele, 1994, fig. 7*a*, *c*). Where they are associated with carbonate alteration (i.e. where the fluids had been highly reactive) these veins have crack-seal micro-textures; if not, they have continuous growth fibres. The fibrous veins are unmineralised, narrow (usually <5 mm) and volumetrically insignificant, and there is no evidence for any direct relationship to gold mineralisation.

The crack-seal fibre veins may show considerable variation in alteration from one side of the vein to the other; for example, in a sample from the Mangana Gold Reef, the wall rock on one side has strong sericite-carbonate alteration, whereas the other side has chlorite-alteration (this shows up on the weathered surface as contrasting red and green colourations). The fibres in this sample show zones formed by repeated cracking during growth, which is typical of the crack-seal process (Keele, 1994, fig. 7*b*). The quartz fibres taper to one side (a more typical feature of quartz comb structures), indicating that they clearly nucleated on the side which contains the more abundant carbonate spotting; such asymmetry may be useful in indicating a direction of palaeo-fluid flow.

Continuous fibre veins occur in the more competent host rocks (i.e. sandstone) which generally show little or no wallrock alteration (Keele, 1994, fig. 7*a*). Although they may contain planar 'Tuttle lamellae' which cut across several adjacent grains in the coarse-grained centres of the veins, they suggest a process of continuous rather than incremental dilation of the rock. Invariably, the fibre veins are cut (and offset) by later veins with coarser grain sizes. The fibres may show evidence of grain boundary movement during recrystallisation, indicating their syn-tectonic nature. The fibrous texture appears to be a remarkably stable one, enabling these veins to remain unaffected by later deformation, with the principal exception being where they occur in the gold-bearing parts of laminated quartz.

Grey quartz

Grey quartz, as its name suggests, is a light to dark grey or bluish form of quartz, usually greasy in lustre. It is generally fine grained and massive or laminated, usually without open space filling or visible crystals.

Finely dispersed rutile, carbonaceous material and fine-grained sulphides (mostly arsenopyrite) give the quartz its characteristic grey colour and suggest that the quartz is probably largely a result of silicification of wallrocks. This quartz is invariably sulphidic and fine grained (Keele, 1994, fig. 7*c*). This could be partly due to the impurities which had the effect of impeding grain growth, or indicates rapid deposition as cherty silica. The massive varieties appear to be the earliest gold-bearing veins, and statistically have the highest grades in the field. The grey quartz may occur as selvages around, and clasts in, white quartz, typified in the Una and Golden Mara mines.

Laminated veins

Laminated quartz veins are characterised by vitreous quartz with banding or laminations parallel to the vein walls. They may contain thin lamellae of wallrock material and/or sulphides, separating quartz domains of varying grainsize. This definition includes the ribbon and stylolite textures of Dowling and Morrison (1989).

These veins are present in a number of localities (e.g. in the Argyle adits, 359-G adit, Brennans adit, City of Hobart); they generally, but not necessarily, occur where the slate is black and probably carbonaceous. The slate is incorporated as thin planar or crenulated laminae of dark wallrock material, separated by grey to white quartz septae that vary from a few millimetres to 15 mm thick (Keele, 1994, fig. 9*b*). The laminated veins are commonly only preserved as selvages to more massive, white, buck quartz veins (e.g. in the Argyle, Pincher, Fingal and Long Struggle mines).

In the Argyle mine, the quartz septae, and to a lesser extent the black laminae, are partially replaced by slightly irregular veins or segregations of a more pure white quartz which is developed perpendicular to the walls (Keele, 1994, fig. 9*c*). At the Argyle and 359-G adits, the laminated veins are from 50–100 mm thick; they occur on the footwall side of the black (?)carbonaceous zone, representing a conduit for fluid that opened up several times during lode formation.

Dark green to grey sericitic laminae, of a similar morphology to the carbonaceous layers described above, are present at the City of Hobart mine. Here, the laminae tend to be developed at the edges of a vein whose centre comprises 30 mm wide massive, fractured grey to white quartz septae.

A stylolitic cleavage in the laminae may be composed of dark residues of sericitic mica, rutile, possibly carbonaceous material, and usually fine-grained arsenopyrite (Keele, 1994, fig. 9*b*, *c*). This cleavage is strongly crenulated where the fill is sericite, otherwise it tends to be wavy in form; the stylolites often separate areas of coarser-grained quartz from finer-grained quartz, indicating active solution transfer during, and as a result of, vein formation. Where fibre veins are present in the laminated quartz, the dark inclusion trails may be traced along the edges of individual quartz fibres, indicating that the fibres and the stylolites were formed during a period of tectonic extension *parallel* to the vein walls (note the difference between the other fibre veins where the extension is *perpendicular* to the walls; Keele, 1994, fig. 7*c*). In one specimen, the laminated grey quartz has a grainsize banding, possibly due to the effect of impurities restricting grain growth, or variation in rates of precipitation.

Macroscopically-visible gold occurs along the grey to greenish quartz bands within laminated quartz (City of Hobart). Although the gold is often intimately related to the arsenopyrite, occurring in the centres of the grains, it may also occur as free grains in quartz.

Folded and boudinaged veins

This type of vein structure is common in lodes which have no clearly identifiable fault surface (Keele, 1994, fig. 8*c*). The faults invariably lack graphitic or carbonaceous material and, therefore, can be classified as brittle-ductile faults or shear zones. Good examples of these come from the Miners Dream, North Eldorado, Old Derby and the Mangana Gold reefs (lower adit). The thin veins are generally ptygmatically folded by the cleavage; at Miners Dream the cleavage consistently dips flatter than the vein, suggesting the possibility of local structural overturning; or else the vein may be 'folded' in the sense that the cleavage is superimposed on an existing non-linear vein geometry (Old Derby). Where the deformation is intense around the lodes, as at Mangana, the veins may be both contorted and boudinaged within the confines of a single lode shear.

Silicified lode

Selected sandstone units within the Mathinna Beds have been locally replaced by silica to form silicified or quartzitic bodies (Linton, North Eldorado, Long Struggle, Mangana Gold Reef and Mount Victoria mines). The quartzite appears to be a more common host to gold veins at Alberton than is the slate. This may be the reason why there are numerous rather relatively short, discontinuous veins of rather variable orientations in this field, reflecting the competency and brittle nature of the host rocks in this area.

Some silicified units contain euhedral or subhedral quartz crystals in a matrix of micaceous lithic material and chert (Linton mine). This style of alteration often appears to have disaggregated some arenites, suggesting that the sediments were poorly consolidated at the time of deformation. The timing of silicification is uncertain.

Ladder veins

Ladder veining may occur in the steeper sections of silicified sandstone beds or in vertical shear zones (Keele, 1994, fig. 8*a*, *d*, 9*e*, *f*). In the North Eldorado adit, steeply-dipping grey silicified beds contain sub-horizontal white quartz veins.

Brecciated quartz veins

Slivers and fragments of wall rock may form as a result of hydraulic brecciation. The breccias contain a wide range of clast types (slate, sandstone, quartz and rarely quartz porphyry and feldspar — usually kaolinised) and sizes. The matrix is also variable from white to grey in colour, and may be carbonate and sulphide-bearing. The brecciated quartz veins occur in most of the gold deposits and may be highly mineralised and gold bearing, but are quite variable in grade. They are a volumetrically important vein type.

At the Golden Gate mine, a 40 mm wide vein contains tabular inclusions of wallrock material which sub-parallel vein walls (Keele, 1994, fig. 9*a*). These inclusions are set in a matrix of coarse-grained white buck quartz. The local jigsaw fit of the breccia indicates its essentially autonomous nature, as well as the very high fluid pressures (above lithostatic) that were locally attained during its formation. These veins are not usually highly mineralised, although they may contain relicts of grey laminated quartz.

Buck quartz

Buck quartz veins have an aggregate of coarse-grained, anhedral quartz grains, white to milky in colour and a vitreous lustre (Dowling and Morrison, 1989). They are commonly barren but may contain some gold. Buck quartz is volumetrically the most important vein type in the field, and normally forms later, but may grade into, grey quartz.

Comb veins

Comb veins are coarser grained than fibre veins, with crystals, identifiable at hand specimen scale, perpendicular to vein walls and partly euhedral. They commonly terminate in cavities and are tapered at their base (Dowling and Morrison, 1989).

In the gold belt these veins are usually wider and volumetrically more important than fibre veins, especially at the Golden Gate mine. They are commonly vuggy, carbonate-bearing, and are typically white in colour. The grainsize varies widely, being usually coarser in the centre of the veins. The veins may also be multiple in form, containing small amounts of sideritic carbonate fill in the outer parts of the vein and ankeritic in the cores; occasionally, a later quartz-carbonate vein, showing a non-fibrous texture, may form on one side of the vein. The quartz in these veins tends to display the effects of later strains (e.g. lattice bending, deformation lamellae etc.) because of their coarse size. Small amounts of coarse-grained sulphide minerals may be present, but the gold content is usually low.

Spider veinlets

These form a random network of fine glassy quartz veinlets, millimetrically sized, which cross-cut host quartz (Dowling and Morrison, 1989). They appear to be partly related to recrystallisation of the highly-stressed earlier quartz veins and are essentially unmineralised (Keele, 1994, fig. 9*b*).

Sulphide veinlets

These rare veinlets are narrow, to about 2 *mm* thick, and are very sulphide rich. They clearly cross-cut all other veins (e.g. Ringarooma United).

Carbonate-rich veinlets

These rare veinlets are narrow, to about 2 mm thick, and are very siderite rich. They clearly cross-cut all other veins (e.g. Golden Gate). They may also form along margins or cores of comb quartz at this location.

Illustrations of vein relationships

At Golden Gate the veins may form networks of orthogonal to oblique cross-cutting sets. The earliest veins are 2–10 mm wide grey fibrous extensional quartz. The cleavage also refracts strongly across the altered selvedges of cleavage-parallel veins. Small-scale movements along the individual cleavage planes suggest that the cleavage is related to an episode of faulting, i.e. the main slaty cleavage forms lazy 's' sygmoidal domains that lie at an angle of 35° to the spaced cleavage. This can be interpreted two ways;

1. Superimposition of one fabric upon another (i.e. S_2 on S_1), or

2. Dextral shear movements along the north-trending faults (i.e. they are C-S fabrics).

A similar tectonic fabric, developed immediately adjacent to the lodes at Mathinna, parallels the nearby north-trending sinistral shears that post-date the quartz lodes. The timing of this cleavage in relation to other events is difficult to assess, however, it may be early-D_3, rather than D_2, in age.

The main cleavage in the northern part of the lineament is a spaced domainal cleavage. At the Mt Victoria mine, for example, the cleavage is defined by an alignment of sericite ± chlorite-rich domains which are separated by 2–3 mm wide quartz-rich bands (Keele, 1994, fig. 9*h*). Evidence that this may be a crenulation cleavage comes from:

1. Early deformed quartz veins which preserve a fibre direction lying at a high angle to the main extension direction, and

2. The main cleavage trending in a northerly direction, which is sub-parallel to the spaced cleavage in the south.

MINERALOGY AND PETROLOGY

Wallrocks

The Mathinna Beds are a poorly sorted, turbiditic siliciclastic sequence, ranging from mica-rich slate through sandy mudstone and argillaceous quartzwacke to quartzite.

Primary textures are poorly preserved, particularly in pelites, but include some lamination and, in arenites, lithic fragments (chert, schist and basalt?). Clasts in arenites are of usually fine to medium-grained, irregular and recrystallised quartz and lithic rocks, with minor potash and plagioclase feldspars; the matrix is mostly fine-grained quartz and muscovite, with minor fine-grained tourmaline, rutile-leucoxene aggregates, zircon, and flakes of detrital muscovite. Much of the matrix has probably been derived from the breakdown of labile lithic material. Chlorite is usually minor but is locally abundant. Stylolites are common and are commonly represented by dark, rutile-rich layers. Some are quartzitic, although this is probably partly related to silicification around quartz veins.

The slates are usually much more sandy and quartz-rich than apparent in hand specimen, but some are highly micaceous to phyllitic or schistose. Chlorite may be abundant. They may be crenulated, with a diamond cleavage. Rarely, some quartz-mica spots are present, probably representing retrogressed andalusite or cordierite in hornfelsed units (Mt Horror Gold mine and Wallis' prospect, Tyne River). Some silty laminae may be present. Graphite is present in some of the more black slate (Golden Gate and Mangana Gold Reef) as small, sporadic flakes usually less than one micrometre thick. Pyrite, arsenopyrite, chalcopyrite and carbonate may be present, usually near quartz veins, and are probably hydrothermal. Amorphous carbonaceous material is probably present but is difficult to confirm. It is probably much of the ultra fine-grained, non-polishable disseminated to diffuse opaque material in grey and black quartz and slate.

Igneous rocks are relatively rare in the gold belt. At Ringarooma United there is a subvolcanic quartz porphyry (probably granite related) and a hornblende-bearing, subvolcanic lamprophyric dyke, both of which are probably fault bounded. The former is partly flow banded and spherulitic, contains quartz veins and stockworks, is pervasively muscovite-altered, and contains some disseminated sulphide (pyrite, arsenopyrite, galena, chalcopyrite and sphalerite) but little gold. In contrast, the lamprophyre appears unveined and unmineralised but is highly weathered and carbonate altered. These rock types have a common spatial relationship to gold mineralisation

(Rock and Groves, 1988). Some silty, pale green rocks in the same mine are quite rich in plagioclase and chlorite, and probably represent basaltic tuff or related epiclastic rocks.

Alteration-related tourmalinites are described below. Chert and some quartzite are vein-related, and are referred to under veining.

Alteration

The only major forms of hydrothermal wallrock alteration noted in the area were silicification and carbonate alteration. The silicification is described under the section on veining. Carbonate alteration is most prominent in the southern part of the field, especially at the Mangana Gold Reef, but can be traced north to the Golden Gate area, always closely associated with mineralised veins. Some is present at Ringarooma United. The main form of this alteration is small rounded porphyroblasts of magnesian siderite (0.1–3 mm) in pelite, but these may be flattened and lenticular in highly sheared slate, suggestive of syn-deformational alteration. The porphyroblasts are prominent in weathered slate due to the small cavities remaining after leaching, but they are sometimes pseudomorphed by limonite. Fine inclusion trails are sometimes curved, sigmoidal or crenulated, which is also consistent with a syn-deformational origin (fig. 2). Irregular aggregates of siderite in arenite also occur but are less prominent. The siderite has an atomic Mg (Mg + Fe) ratio of about 0.35–0.45, similar to the chamosite-rich chlorite in these rocks, suggesting that it has probably replaced this phase. Some possible reactions are:

(1) Chlorite → siderite + muscovite

$$13H^+ + 15HCO_3^- + 3(Fe,Mg)_5(Al_2Si_3)O_{10}(OH)_8 + 2\,K^+ \rightarrow 15(Fe,Mg)CO_3 + 2KAl_3Si_3O_{10}(OH)_2 + 3SiO_2 + 24H_2O$$

(2) Chlorite + K-feldspar → siderite + muscovite

$$5H^+ + 5HCO_3^- + (Fe,Mg)_5(Al_2Si_3)O_{10}(OH)_8 + KAlSi_3O_8 \rightarrow 5(Fe,Mg)CO_3 + KAl_3Si_3O_{10}(OH)_2 + 3SiO_2 + 8H_2O$$

(3) Chlorite + quartz → siderite + pyrophyllite (as a component to muscovite)

$$5H^+ + 5HCO_3^- + (Fe,Mg)_5(Al_2Si_3)O_{10}(OH)_8 + SiO_2 \rightarrow 5(Fe,Mg)CO_3 + Al_2Si_4O_{10}(OH)_2 + 8H_2O$$

There is no good evidence for sulphidation of the wall rocks, although some minor arsenopyrite and pyrite are present in slate and quartzite, particularly in some stockworks and silicified areas (e.g. at the Mt Victoria and Mercury mines). Some pyrite is also present in slate around Mangana and Mathinna, with no close relationship to veining. The arsenopyrite in wallrocks is, in part, poikiloblastic with quartz inclusions, and may exhibit pressure shadows.

Tourmalinites are rare but present at Gorge Creek, where they may be almost pure, brown tourmaline (10–50 µm in size) but usually contain abundant quartz and minor biotite. Their extent is unknown, but they appear closely related to the Au-W-As-Cu bearing quartz veins. Carbonate-altered pelite at Wallis' prospect contains abundant disseminated tourmaline (~1%), probably also related to granitic activity.

Veins

Quartz veining in the Mathinna Beds is complex and variable, and is taken here to encompass some cherts, silicified sediments and cataclasites, breccias, stockworks and other related siliceous rocks. Carbonates, sulphides or silicates may dominate some veins, but these are usually small and minor. The true quartz veins observed include buck, comb, fibre, laminated (ribbon), breccia, spider veinlets and grey quartz (Dowling and Morrison, 1989). They vary from microscopic to many metres in thickness, and may be straight walled, ptygmatic or boudinaged. Silicified units are described as cherts below. Up to five stages of quartz can be visible in one thin section (e.g. at Mt Victoria).

Buck quartz is the most common variety, in white to milky quartz veins, and is usually unmineralised. It grades into comb quartz, sometimes containing vugs. The vugs are commonly related to the latest stages of veining, and are often glassy to transparent, with rare crystals from 0.1 mm to 50 mm. In thin section the buck quartz veins are usually coarse grained, stressed and brecciated, partly annealed by recrystallised cherty to medium-grained quartz as spider veinlets. Sulphides and carbonates may be present locally in comb quartz (see below), and some kaolinite patches indicate pre-existing feldspars (e.g. at the Mangana Gold Reef mine). The feldspars may be rarely preserved (e.g. at the Mercury mine). Where carbonates are present, the selvages are typically siderite, and the cores ankerite-dolomite rich. The buck quartz sometimes grades into stockworks and breccias, and may have selvages or clasts of laminated and/or grey quartz.

Fibre veins are small and minor, are apparently unmineralised, are sometimes chloritic, and may form apophyses on other veins.

Laminated veins are important as a major gold host (see the geochemistry section). They may be grey or white but commonly contain both varieties, the grey predominantly on selvages but also in vein cores. They contain thin laminae of fine-grained micaceous or black slaty material, which may host visible gold. Crack-seal laminae and stylolites may also be present, and all of these structures are rich in fine-grained residual material resulting from replacement or disaggregation of the host rocks (fig. 3). Arsenopyrite is a very common constituent, and may be very fine grained (fig. 3) but may also be macroscopically visible. Fine-grained rutile is also locally abundant, as is mica. The black and grey colours are thought to be due to these minerals, and although graphite is very rare, some amorphous carbonaceous material may also be present, but could not be confirmed. The veins have formed by repeated failure and fluid injection at the vein/slate contact, where veins parallel slaty cleavage.

Breccia veins are variable in nature, but typically contain slate or psammite clasts in quartz. Other variants are white quartz clasts in a grey quartz matrix or vice versa, and quartz in a fine-grained, soft greyish micaceous matrix. Vein formation was complex, with repeated formation and destruction of veins in some areas. These veins are partly cataclasites, with mortar textures and are variably mineralised, but tend to be poorer in grade than the laminated veins. Sulphides are sometimes macroscopically visible.

Figure 2

Carbonate porphyroblasts in pelite, showing sigmoidal, rotated and crenulated inclusion trails, in C103823. Plane polarised light. Field of view: 4.4 × 3.0 mm.

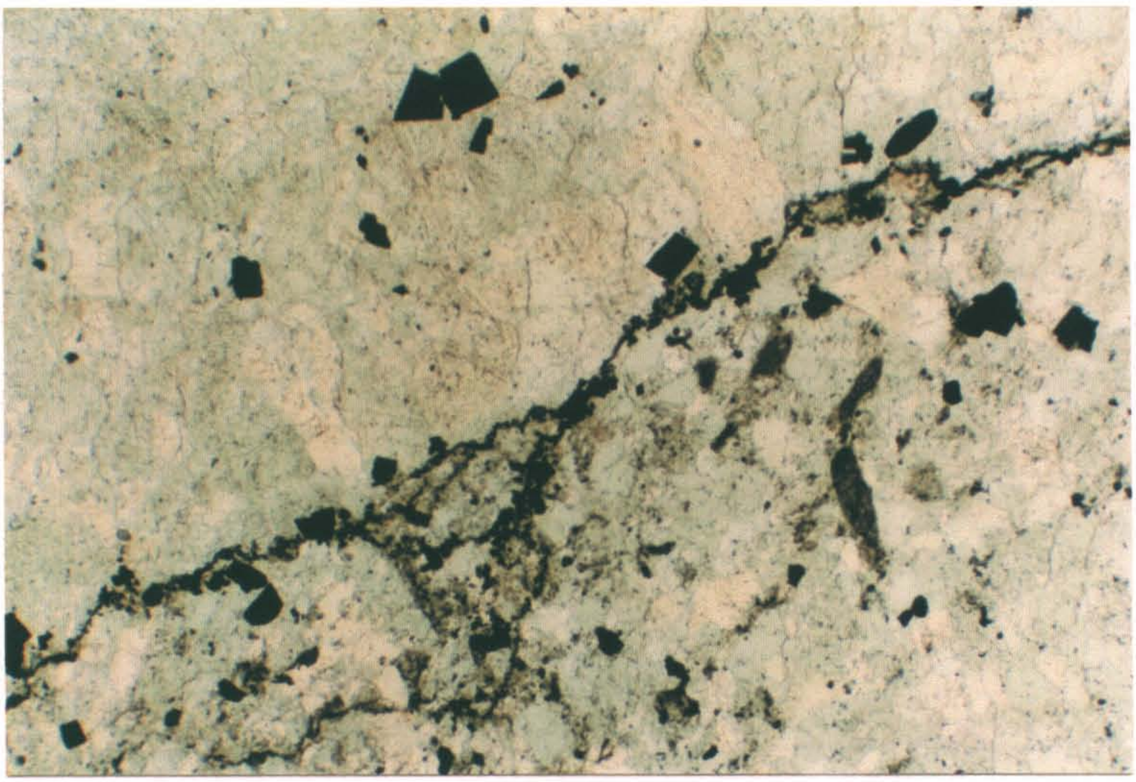

Figure 3

Laminated quartz, showing stylolites, arsenopyrite and fine relicts of slaty material in C103879. Plane polarised light. Field of view: 1.8 × 1.2 mm.

5 cm

Grey quartz is usually found in laminated veins, but sometimes forms simply as a selvage or as irregular fragments in veins. It is one of the most consistently gold-rich styles of vein but is locally unmineralised. The texture is always fine to very fine grained, cherty to quartzitic, and may be streaky, laminated or massive. The veins weather to a brown, quartzitic appearance. In thin section the textures are variable, typically cataclastic and containing a range of very fine to medium-grained particles including probable early (white buck or comb?) quartz grains and aggregates, and commonly late, relatively unstressed white or glassy spider or comb veinlets (fig. 4*a*). Subhedral, elongate quartz crystals of random orientation are a common constituent, giving a 'woodpile' texture (fig. 4*b*). These may relate to replacement or assimilation. Grey quartz contains moderate amounts of very fine-grained arsenopyrite and/or rutile, giving the dark colour, although sulphides are rarely macroscopically visible. Fine-grained mica, chlorite and carbonate may also be present.

Chert, quartzite and silicified rocks

Local silicification has affected the wallrocks in some areas, for example at Mt Victoria. Here there are some dark grey arsenopyrite-bearing quartzites with minor quartz veining but low gold values. In thin section there is abundant micro-veining and brecciation. In some rocks, which apparently were poorly consolidated during deformation, there has been complete disaggregation (e.g. Linton) producing an impure, very inhomogeneous, micaceous cherty rock with coarser clasts of angular, polycrystalline to euhedral (fine to medium-grained crystals) quartz. They appear to be arenite or siltstone in hand specimen, but are apparently silicified cataclasites or fault gouge (the assimilation quartz of Dowling and Morrison, 1989).

Vein-forming minerals

Carbonates

Siderite and dolomite-ankerite are common in veins in the Golden Gate mine, often as coarse-grained, late-stage vug-fillings with minor sulphides. The carbonate typically grades outward, with an increasing Mg/Fe ratio, from ankerite to ferroan dolomite. The carbonates are similar in appearance when fresh, but the siderite weathers to a red and the ankerite to a cream colour. Similar carbonates also occur in the Mangana Gold Reef and other deposits, but are rarely abundant.

Silicates

Chlorite and muscovite are sporadically present in some veins, particularly near wallrock contacts. The compositions are similar to those in the wallrocks, and are discussed further under thermobarometry. The mica is probably largely remnants of replaced and disaggregated wallrocks, but some massive selvages and veinlets may indicate local sericitisation. Chlorite may occur in coarse aggregates or as vermicular intergrowths with quartz in some veins, giving the veins a green colour, or in separate fine veinlets. Fresh feldspar is uncommon (but verified at the Long Struggle), but common, sometimes coarse, kaolinite clasts probably indicate its former local abundance at the Mangana Gold Reef.

Sulphides

Sulphide minerals in the veins are dominated by arsenopyrite, with sporadic pyrite and minor to rare galena, chalcopyrite, tetrahedrite, sphalerite, galena and bournonite. Some late-stage sphalerite is relatively iron-poor (1.4–3.6 wt% Fe), which is typical of that in gold-enriched sulphides deposited from relatively low temperature (<300°C) hydrothermal fluids (Hannington and Scott, 1989). The significance is uncertain in these deposits.

Few indications of paragenetic relationships are evident, and the sulphides and gold most likely crystallised simultaneously. Elongate pyrite pseudomorphs in some samples may have replaced pyrrhotite (Golden Gate and Ringarooma United), and pyrrhotite inclusions occur in pyrite in the Mercury Mine and Ringarooma United. The presence of pyrrhotite indicates that conditions were originally relatively more reducing or sulphur poor. Galena veinlets in arsenopyrite indicate some late-stage remobilisation during deformation or a later stage of lower temperature mineralisation following brecciation. Fine-grained arsenopyrite is particularly prominent in some of the blue and grey quartz, especially in stylolites. Chalcopyrite occurs as inclusions in some arsenopyrite and pyrite, possibly indicating relatively early formation.

Other minerals

Apatite has been noted rarely in the veins. Rutile is very common, ranging from very fine to medium grained. It is particularly prominent in some of the blue and grey quartz, especially in stylolites. It probably represents original material left after silicification and replacement of wallrocks. Graphite is rare but is present in quartz veinlets in some black slate at Golden Gate and Mangana Gold Reef.

Gold mineralogy

Gold was not macroscopically or microscopically observable in the great majority of samples examined, despite some moderate to high grades. This is probably due to the 'nugget effect', where gold is erratically distributed as rare but relatively coarse grains which makes correlation of petrographic and analytical results difficult. Nevertheless, a number of samples did contain visible gold, usually microscopic but sometimes as grains to about 1 mm in size. These were found at the Linton, Pincher and Strickland mines. Gold-bearing samples used in the study of deposits in this area by Threader (1967) were also examined, revealing numerous gold grains. The quartz hosting visible gold varies from non-sulphidic white quartz to sulphidic, mottled grey and white quartz.

The alluvial workings at Mangana contain some gold grains up to 5 mm or more in size, and Twelvetrees (1907) indicated that some nuggets, variously described as up to 7 or 11 oz (0.2–0.3 kg), were recovered. Some apocryphal stories from older residents at Mathinna relate how some samples from the Golden Gate mine were so rich in gold they could be "twisted like rope". However, fine-grained gold appears to be typical of northeastern Tasmania.

The gold grains observed in this study range in size from probably sub micron to about one millimetre. Shapes, textures and parageneses are quite variable, and include:

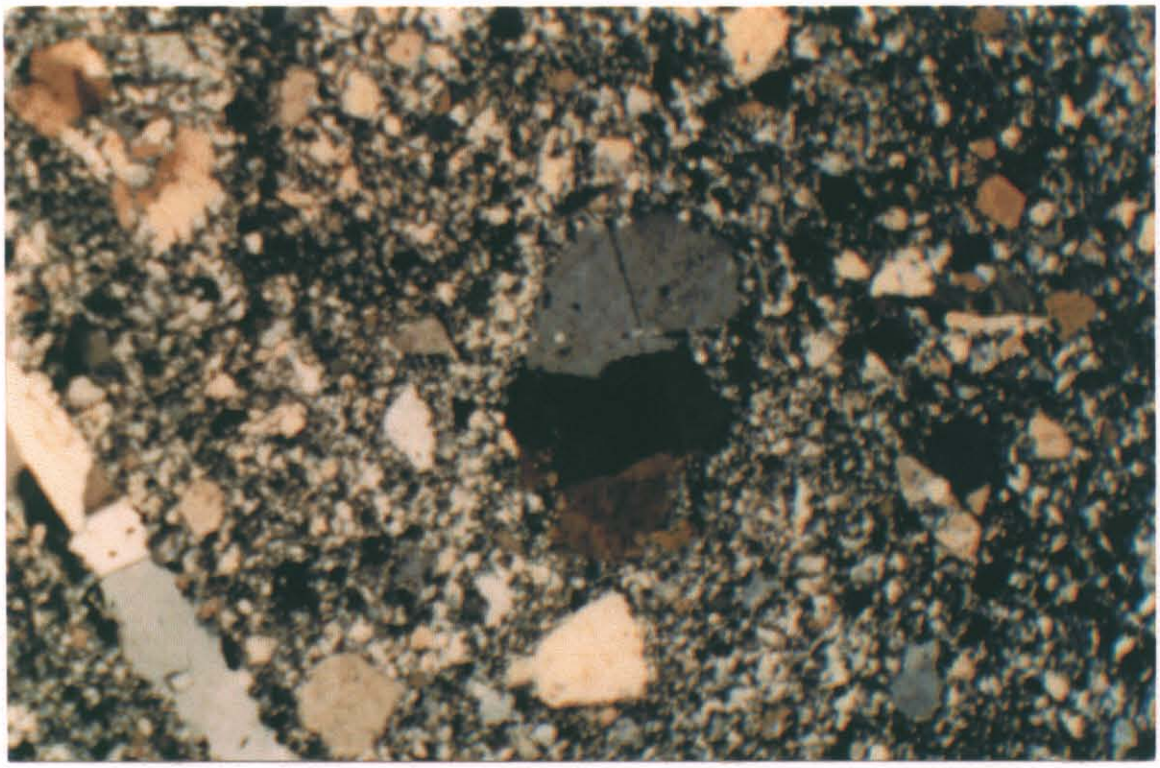

Figure 4a

Grey quartz, showing inclusions of early coarse grained quartz in a cherty matrix, cut by late stage veinlets, in C103811a. Cross polarised light. Field of view: 4.4 × 3.0 mm.

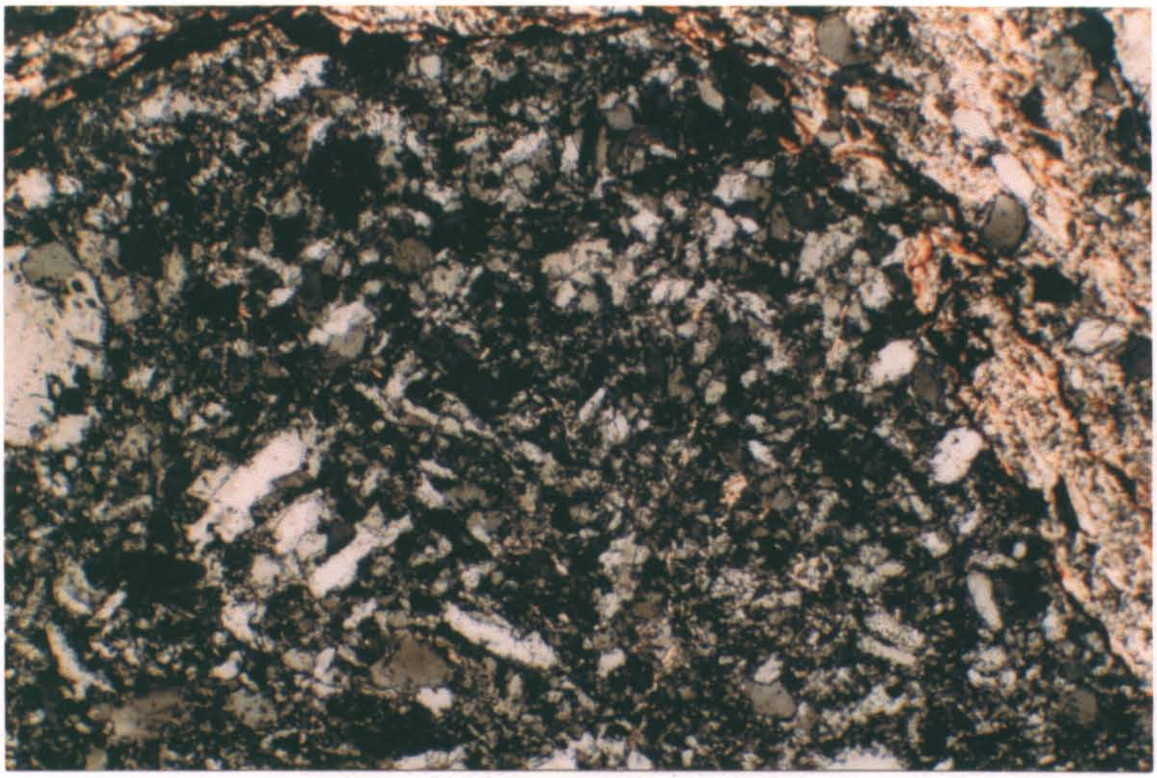

Figure 4b

Grey quartz, showing 'woodpile texture' of subhedral quartz crystals in a cherty matrix, in C1038234. Cross polarised light. Field of view: 1.8 × 1.2 mm.

5 cm

- equant inclusions in quartz, ~1–100 µm (fig. 5, 6). Some gold is in grey quartz patches in white quartz, the grey colour possibly due to fine inclusions of rutile(?) and carbonaceous material(?).

- fine to medium-grained veinlets in quartz and slate (fig. 6).

- large irregular blebs associated with quartz and arsenopyrite. Arsenopyrite sometimes appears to be replacing gold, although the relationship is unclear (fig. 7).

- small inclusions in arsenopyrite.

- micro-veinlets in coarse, brecciated arsenopyrite, in some cases associated with galena veinlets (fig. 8).

- intergrowths with secondary lead-aluminium arsenates (?philipsbornite, probably pseudomorphing a sulphide).

- intergrowths with goethite (probably pseudomorphing pyrite) (fig. 5).

The gold appears to have crystallised prior to and/or simultaneously with quartz, pyrite and arsenopyrite, as indicated by the small inclusions in these minerals. The textures have probably been partly modified by later deformation, remobilisation and recrystallisation. There is no evidence for secondary enrichment of gold, although some gold may have been released from sulphides during weathering. The gold surrounded by arsenopyrite in one section is enigmatic, but probably represents some form of replacement. Replacement of gold by arsenopyrite seems unlikely. Perhaps an unknown mineral was partly rimmed by arsenopyrite, then dissolved and the cavity filled by gold. Alternatively a metastable Fe ± As mineral may have been removed simultaneously with gold precipitation.

Gold composition

The composition of gold grains is relatively consistent, with high fineness, about 926–993, with the exception of some gold from the Linton mine, with fineness about 654–661 (Table 6). The higher fineness range is consistent with gold deposited in the higher temperature class of mesothermal deposits, as noted by Antweiler and Campbell (1977), which average about 900 in fineness. Deposits in contact metamorphic, pyro-metasomatic and hypothermal deposits have similar, high fineness. The gold (electrum) at Linton is closer in composition to those in the lower temperature part of mesothermal deposits, which average about 777 in fineness (Antweiler and Campbell, 1977). Gold in epithermal deposits have a similar composition. The low fineness of gold has also been taken as an indication of a magmatic origin (Peters *et al.* 1990), although no other indication of this is present in the Linton deposit. The veins strike about ENE, different from most in this 'gold belt' but similar to many granite-related veins at Scamander and in other areas of northeastern Tasmania (Groves, 1972). The high fineness of gold in the Mt Horror As Prospect is anomalous with its apparent granite association.

Investigation of concentrates from Linton actually reveal the gold to be bimodal in composition, with a small proportion of high purity grains. Their significance is not understood, and they may be derived from extensive weathering and silver leaching, or they could represent an earlier, higher temperature mineralisation phase. No compositional zoning of gold grains has been observed in these samples. Mercury contents show no systematic variation, except for being high in the silver-poor Jubilee sample. This sample is in white quartz only, possibly indicating a different origin to the other analysed samples, associated with grey quartz.

Table 6

Gold analyses

Sample No.	Location	Grain	Au	Ag	Hg	Fineness
103880	Linton	Au1	66.0	34.4	0.1	657
103880	Linton	Au2	65.1	33.4	0.3	661
103880	Linton	Au3	64.1	33.9	0.2	654
VMT 5	Mt Victoria	'Au, core'	73.4	2.4	0.1	968
VMT 5	Mt Victoria	'Au, rim'	96.9	3.2	0.2	968
VMT 5	Mt Victoria	Au rim 2	96.4	3.4	0.0	966
VMT 5	Mt Victoria	Au core 2	96.0	3.3	0.1	966
VMT 5	Mt Victoria	core 3	96.2	3.3	0.1	967
VMT 5	Mt Victoria	rim 3	97.1	3.4	0.0	966
VMT 23	Mt Horror As lode	Au1	94.2	5.7	0.3	943
VMT 23	Mt Horror As lode	Au2	95.5	6.1	0.2	940
VMT 23	Mt Horror As lode	Au3	96.1	6.1	0.0	940
VMT 22	Gladstone	Au1 core	92.9	7.4	0.2	927
VMT 22	Gladstone	'Au2, rim'	92.9	7.4	0.0	926
VMT 20	Golden Entrance	Au 1	94.5	5.0	0.1	950
VMT 20	Golden Entrance	Au2	95.4	4.8	0.0	952
VMT 20	Golden Entrance	Au3	92.3	5.1	0.1	948
VMT 17	Jubilee	Au1	102.5	0.8	1.0	992
VMT 17	Jubilee	Au2	90.8	0.8	1.1	99
VMT 17	Jubilee	Au3	90.6	0.6	0.9	993

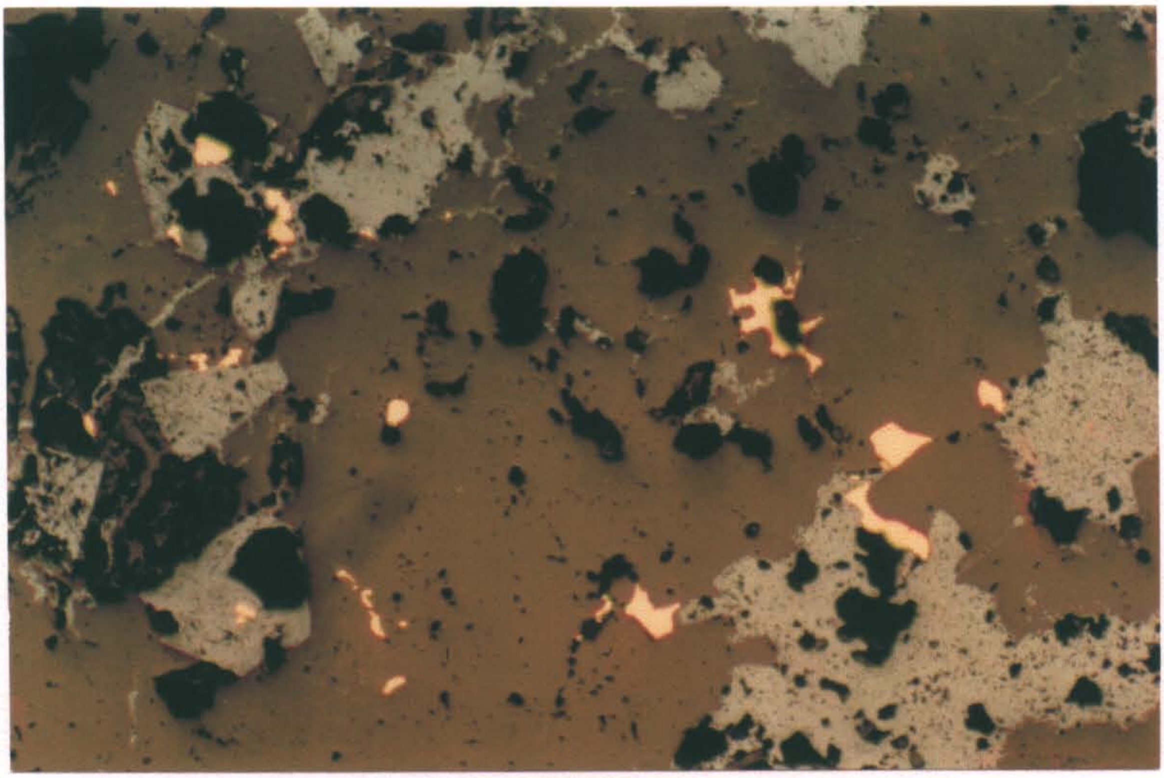

Figure 5

Gold in goethite (pseudomorphing sulphides) and quartz, in VMT23.
Plane polarised reflected light. Field of view: 2.2 × 1.5 mm.

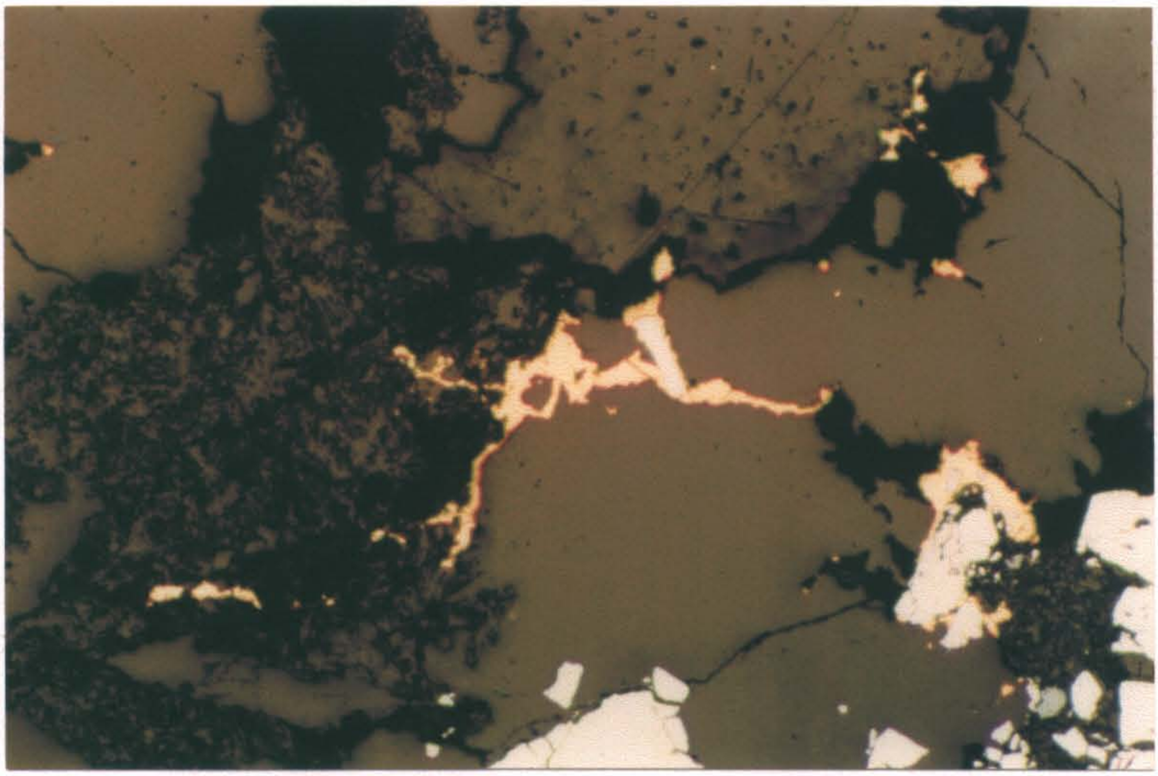

Figure 6

Gold in microveinlets and fine inclusions in slate and quartz, in VMT5.
Plane polarised reflected light. Field of view: 2.2 × 1.5 mm.

5 cm

Figure 7

Gold in coarse grains rimmed by arsenopyrite and pyrite, in VMT20.
Plane polarised reflected light. Field of view: 2.2 × 1.5 mm.

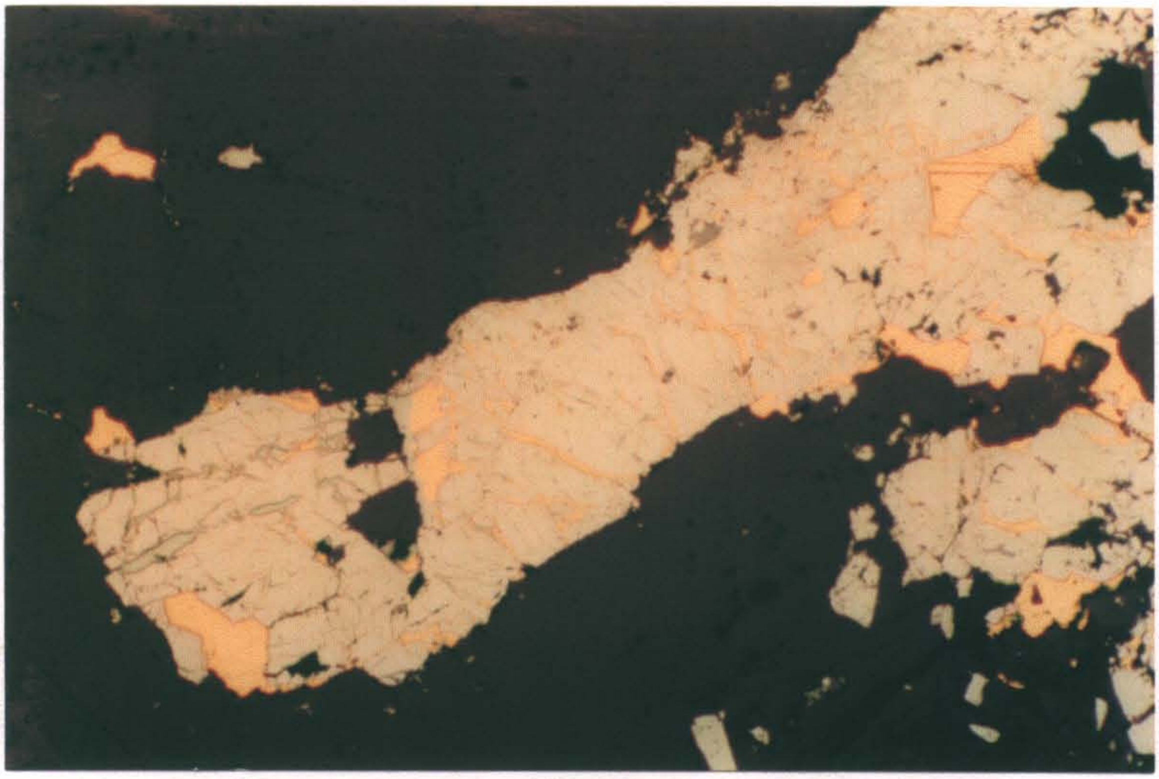

Figure 8

Gold in microveinlets with galena in arsenopyrite and as inclusions in quartz, in VMT5.
Plane polarised reflected light. Field of view: :2.2 × 1.5 mm.

5 cm

Gold in sulphides

A number of arsenopyrite and pyrite grains from several different deposits were analysed for trace gold, with several significant values being noted, the highest being about 310 ppm in arsenopyrite from Mt Victoria and 770 ppm in pyrite from Linton. The lack of reproducibility in these results, however, is more consistent with the presence of submicroscopic gold grains (as described by Mao, 1991) rather than gold being present as a solid solution within sulphides Cabris *et al.*, 1989; Cook and Chryssoulis, 1990). Boiron *et al.* (1989) noted the enrichment of gold in microcracks and peripheries of arsenopyrite, and so more detailed studies may be required here. Wu *et al.* (1990) noted gold-bearing arsenopyrite in synthetic and some natural samples as being relatively fine grained and needle-like, but arsenopyrite of this form was not studied here.

Chlorite and Muscovite Thermometry

Chlorite compositions, based on the Cathileneau and Nieva (1985) thermometer, indicate temperatures of between 280 and 320°C in both veins and groundmass in the Golden Gate slate.

Some muscovites in slate and veins were analysed and used for temperature estimates using the Cathileneau and Izquierdo (1988) method. These indicated temperatures of between 290 and 320°C in the Golden Gate slate (groundmass and detrital mica) and veins. These temperatures are almost identical with the fluid inclusion temperatures reported in this paper, and indicate extensive re-equilibration of wallrocks with the vein-forming fluids.

Mica compositions from the Mangana gold reefs, however, give variable temperatures that range between 150 and 290°C. These may indicate some lower temperature alteration or partial resetting during weathering, and further study is needed. Some chlorites at Alberton give erratic and low temperatures, reflecting unusual, aluminium-rich compositions (sudoites or smectite-chlorite intergrowths?). These may be a reflection of weathering or local phyllosilicate formation at silica activities undersaturated with respect to quartz.

ILLITE CRYSTALLINITY

Introduction

Eighty pelite samples were collected throughout the Mangana–Forester gold belt for illite crystallinity (IC) studies, to give an indication of variations in metamorphic grade. The illite crystallinity method is an X-Ray Diffraction (XRD) technique for determination of the relative degree of crystallinity in the muscovite-illite series, using the 10 Å (001) peak width (PW). The PW values in nature range from about 0.08° in 2θ angle (highly crystalline muscovite) to 0.5° 2θ (poorly crystalline illite). This can give an indication of subtle variations in metamorphic grade. Other studies of IC in slate terrains show systematic spatial variations. It was also hoped to relate IC variations to hydrothermal alteration associated with gold mineralisation. Detailed IC measurements in fresh drill hole samples near Mathinna are closely related to magnetic susceptibility, and apparently reflect a hydrothermal overprint (Bottrill, in prep.)

There are a number of variations of the technique, but we have basically followed most of the recommendations of Kisch (1991). One exception to this is with sample loadings, where Kisch has recommended loadings of at least 3 mg/cm^{-2} to maximise peak heights, whilst Krumm and Buggisch (1991) recommend less than 0.25 mg/cm^{-2} to maximise reproducibility in peak width. As a compromise we have run our samples at loadings of about 1 mg/cm^{-2}, although it has varied somewhat from about 0.5 to 1.5 mg/cm^{-2}. With our samples, instrumentation, techniques and settings, we appear to get reasonable reproducibility below 1.5 mg/cm^{-2}. Instrument settings are: Philips generator PW1729/goniometer PW1050/25, Cu Ka, 40 kV, 30 mA, normal focus tube, graphite monochromator, Ni filter, slits 1°/0.2 mm/1°, xenon proportional counter (PW1752/00), time constant = 5 sec, scan rate = 0.6° 2θ /min, and chart speed set so that 1° 2θ equals 40 mm on the chart.

Some standards prepared by H. J. Kisch were used to recalculate the measured values. Regression analysis of the five standard samples indicates that our peak widths are a factor of 1.39 higher than the standards ($R^2 = 0.985$). The precision and accuracy of the method was not determined independently, but was described by Blenkinsop (1988) as ranging between 1.3 and 7% and 3 and 10% respectively. Reproducibility is usually in the 0.01–0.02° 2θ range.

The true PW values in these samples are probably complicated by at least four factors; detrital mica content, degree of weathering, retrograde metamorphism and probably hydrothermal alteration. Attempts are being made to relate these factors to PWs.

Results

The results are listed in Appendix A. In summary, there is a range in corrected peak widths of 0.24–0.31 (± 0.01), average 0.264° 2θ. This would put all of the samples within the lower anchizone (lowest grade metamorphic zone, PW = 0.21–0.38° 2θ), as defined by Kübler (Kisch, 1991). The presence of kaolinite and smectite in many samples is indicative of diagenetic grades, but again this is probably a weathering feature.

About half (46) of the samples were checked for mineralogy by XRD; eighteen of these contained moderate amounts of kaolinite and several contained minor smectite. These samples are commonly surface samples, soft, discoloured and weathered in appearance, although some are black and reasonably hard and fresh looking. The average PW is 0.252° 2θ for 28 fresh samples and 0.265° 2θ for 18 weathered samples. Where both weathered and fresh samples have been collected at one site, the weathered sample is about 0.02° 2θ higher in PW (Mt Horror Gold mine and Majors Gully).

Although the samples are prepared as sedimentation mounts to give a clay fraction, there is still a possibility that samples with coarse detrital mica (e.g. micaceous sandstone) have relatively low PWs. The two tested here average 0.26° 2θ, i.e. just below average.

The hornfelsed samples tested to date show, somewhat surprisingly, a large range of PW values (0.25–0.29, average of five 0.272° 2θ) suggesting that they may have been partly retrogressed (e.g. sericitisation of aluminosilicates and feldspars) following contact metamorphism. This may overlap with weathering in its effect.

In many of the samples examined, by both XRD and petrography, quartz veining, carbonate alteration, silicification, or other indications of hydrothermal alteration are apparent. Muscovite/phengite is an important alteration phase in other mesothermal gold deposits (Boiron *et al.*, 1989; Peters *et al.*, 1990), and is suspected but has not been confirmed here. These forms of alteration are probably in part associated with gold mineralisation, and commonly intersect or overprint illite or mica-rich lithologies. The thermal variations associated with these alteration events could be expected to also overprint illite crystallinities set by the regional metamorphism. Five quartz-veined samples averaged 0.266° 2θ, i.e. quite average, but ten carbonate-altered samples averaged 0.255° 2θ, slightly low.

Even allowing for the presence of signs of weathering, hydrothermal alteration, detrital mica, etc., it has not been possible to find conclusive evidence for any systematic variation from east to west. This is in contrast to the findings of Taylor (1992), whose samples show distinct geographical groupings: 0.26–0.31° 2θ west of Catos Creek Dyke (i.e. nearer Mathinna) and 0.29–0.35° 2θ east of the dyke (nearer Scamander). Our samples closely match his western group, which were collected adjacent to our area of study. His samples may also be effected by weathering, hornfelsing and alteration overprints, although this was not recorded, but the gross variation is probably real.

There may be some significant variation in PW from north to south; the non-hornfelsed samples to the north of Ringarooma (Linton and Golden Mara) generally show higher PW values (0.25–0.29° 2θ, average of seven 0.28° 2θ) than those in the south. The values are slightly lower (0.25 and 0.27° 2θ) at the Mt Horror Gold mine in the same area, but this is probably due to hornfelsing. Many of the pelites collected in the north were weathered and kaolinised (as shown by XRD), but where fresh (e.g. non-kaolinised underground samples) are still relatively high in PW.

The Una and Strickland samples are also rather high in PW for fresh samples (0.27–0.28, average of four 0.272° 2θ). More detailed studies are needed to confirm such results, and may reveal more subtle variations over the area. Some relatively low values at the Sunbeam mine and Tower Hill mine (0.24° 2θ) are inexplicable, unless they are affected by contact metamorphism due to Jurassic dolerite or other intrusions.

Conclusions

The results from this preliminary study of the Mangana–Forester area suggest that there is some systematic variation in IC relative to location and carbonate alteration. IC seems to be lower (i.e. higher PW) in the Linton, Warrentinna and the Una-Strickland areas. Carbonate alteration is related to higher IC (lower PW), but quartz veining is not systematically related. Trends are complicated due to the problems involved in collecting unweathered (based on XRD), non-hornfelsed, pelite-rich rocks. Some of the regional variations may reflect more complex geological structures, or result from widespread but variable hydrothermal overprinting. There should be some useful applications in association with more detailed geological mapping and detailed traverses, if applied with care. It is important in future studies to carefully note signs of hornfelsing and weathering, especially as indicated by kaolinite and smectite, in order to obtain reliable results.

FLUID INCLUSIONS STUDIES OF SOME QUARTZ VEINS FROM DIFFERENT GOLD MINES AND PROSPECTS

Introduction

The following preliminary fluid inclusion study was carried out on quartz samples from 22 different gold prospects in northeast Tasmania and two barren quartz veins (along the Mangana–Rossarden and the Upper Esk Roads) (Appendix 3). Over 100 unpolished thick sections (150 to 400 μm thick) and 33 doubly polished sections were prepared for fluid inclusion petrography and microthermometry studies. However the short term nature of the project prevented the collection of systematic microthermometric measurements for all the visited prospects and the gathering of statistically more reliable data.

The purpose of the investigation was to:

(a) identify different generations of early-formed fluid inclusions in different quartz types; particularly to compare grey and white quartz veins.

(b) establish the chemical composition and temperature of the ore-forming fluid and to investigate whether there were any variations in these parameters between different prospects; and

(c) calculate oxygen isotope compositions of mineralising fluid using microthermometric data and oxygen isotope values of different quartz types. The results may then be interpreted to identify probable ore-fluid sources.

Due to the effect of different phases of deformation on the fluid inclusions, the standard criteria used for distinguishing primary from secondary fluid inclusions (Roedder, 1984) cannot be applied readily in deformed rocks, and it may be more appropriate to use terms such as 'early formed' or 'primary looking' for those which appear to be as primary fluid inclusions in a deformed mineral. This is particularly true if the history of the evolution of metamorphic fluid cannot be well established.

Most of the early-formed fluid inclusions have been destroyed by extensive fracturing, brecciation and recrystallisation in that the sections are mainly covered by trains of very small late (secondary) fluid inclusions. This is a characteristic feature in the majority of the sections prepared from the Alberton goldfield where only small, early-formed fluid inclusions survive. Some fluid inclusions adjacent to sulphide grains also appear to have been protected from the effect of brecciation, recrystallisation and other physical changes (e.g. necking down, leakage or overprinting by later low-temperature fluid inclusions). Fluid inclusions are rare in some of the sections, as the deformation appears to have caused the migration of inclusions to sub-grain boundaries. Thick sections prepared from the southern part of the field appear to contain more and larger, early-formed, fluid inclusions. Most of the sections are characterised by having myriads of tiny fluid inclusions along healed microfractures, cutting across the grain boundaries. This texture is known as wispy or brushy texture and appears to be indicative of deep environments, greater than 4 km depth (Reynold, 1990).

Every attempt was made to use only the early-formed (primary or pseudo-secondary) fluid inclusions for microthermometric measurements.

The microthermometric results are shown in Appendix 3. The following terms and abbreviations are used throughout this section:

L Liquid
V Vapour
I Ice
M melting point
C Clathrate melting point
Th Homogenisation temperature of fluid phases:
ThL = L + V ⇒ L
(i.e. fluid inclusions homogenise to liquid)
ThV = L + V ⇒ V
(i.e. fluid inclusions homogenise to vapour)

The microthermometric measurements were conducted at the fluid inclusion laboratory at the Resource and Exploration Development Branch, Department of Development and Resources, Tasmania.

Description and Classification of Inclusions

Fluid inclusions in quartz have a variety of shapes (rounded, negative crystal or irregular) and range in size from <3 to >50 µm, with the majority being in the range of 3 to 10 µm.

Early-formed fluid inclusions may be classified into two different types according to their appearance at room temperature:

Type A: Carbon dioxide-bearing fluid inclusions, consisting of CO_2 as vapour or vapour + liquid and LH_2O is not visible (A1) and $H_2O + CO_2$ as $LH_2O + V(H_2O + CO_2)$ (A2) or $LH_2O + LCO_2 + V(H_2O + CO_2)$ (A3).

Type B: Two phase $(L + V)H_2O$ early-formed or primary fluid inclusions.

Type A:

Type A inclusions are the most common fluid inclusions and can be seen in both grey and white quartz veins. They vary in size from <3 µm, where different phases cannot be seen clearly, to <50 µm. Type A1 fluid inclusions may contain a single liquid phase at room temperature and vapour CO_2 nucleates upon cooling of the fluid inclusions (i.e. higher density and internal pressure). This is also true for some of the type A3 inclusions, where the CO_2 vapour bubbles appear only on cooling. The relative abundance of the different types of type A inclusions in different samples is not known, as only very few sections have been used for microthermometric measurements.

Type A2 fluid inclusions are associated with type A1 inclusions. Type A2 inclusions consist of an aqueous solution and a vapour bubble with a very dark meniscus around the vapour bubble. The occurrence of CO_2 can only be identified by freezing experiments (i.e. melting of solid CO_2 phase).

Type A3 inclusions consist of aqueous solution and a $CO_2 + H_2O$ vapour bubble ringed by liquid CO_2. They are commonly rich in CO_2, being more than 50% by volume, and exhibit similar phase ratios in the same section. Type A fluid inclusions belong to the same generation of fluid, as the inclusions occur in close association with each other and often can be observed in the same grain under the microscope. The fluid inclusions appear to contain less CO_2 in white quartz veins which formed in the last stages of quartz deposition (e.g. sample 107260).

Type B

Type B fluid inclusions were observed only in samples from the Gorge Creek Tungsten prospect (sample 107141), in samples from the Rossarden–Mangana Road (sample 107189), and from euhedral quartz crystals grown in vugs (sample 107212). They show different shapes and the vapour-liquid ratios are relatively low (~10 to 30% by volume). Secondary fluid inclusions were not used for microthermometric measurements. Solid anisotropic inclusions were observed in few fluid inclusions from the Gorge Creek Tungsten prospect.

Fluid Inclusion Homogenisation Data

A high proportion of the CO_2-rich fluid inclusions decrepitated on heating before they homogenised. This is a common phenomenon in the CO_2-bearing inclusions because of the internal pressures generated during heating. Fluid inclusion homogenisation temperatures obtained for type A and B fluid inclusions from Mangana Gold Reef, West Miami, Argyle, O'Brien, Strickland, Crown Prince, Miner's Dream, Gorge Creek Tungsten and Linton prospects, the Rossarden–Mangana and Upper Esk roads are shown as histograms in Figure 9.

Homogenisation temperatures for type A1 fluid inclusions range from 16.5 to 28.0°C. They homogenised either to liquid or vapour phase.

The final homogenisation temperatures for A2 and A3 fluid inclusions range from 245 to 355°C, with the majority being in a narrow range of 280 to 320°C. No systematic variation in homogenisation temperatures or compositions of the fluid inclusions appear to exist along the belt between Mangana and the Forester goldfield. However it should be noted that this interpretation is based on a limited number of microthermometric measurements on few sections, and needs to be backed up with more systematic microthermometric data.

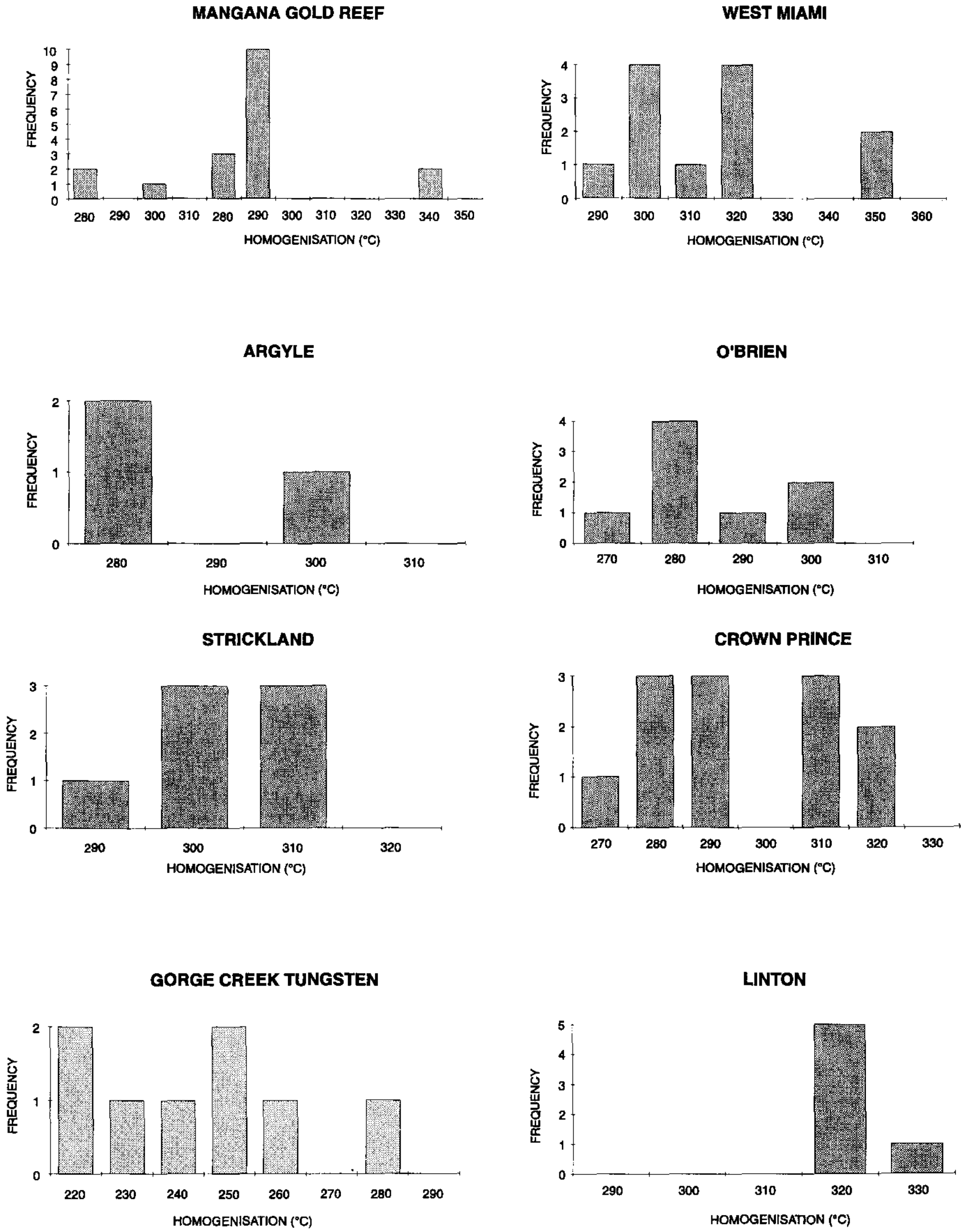

Figure 9

Homogenisation temperature histograms for Types A and B fluid inclusions, for indicated prospects and locations

5 cm

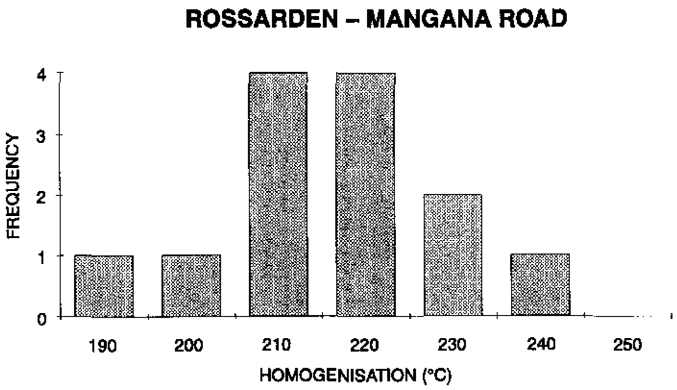

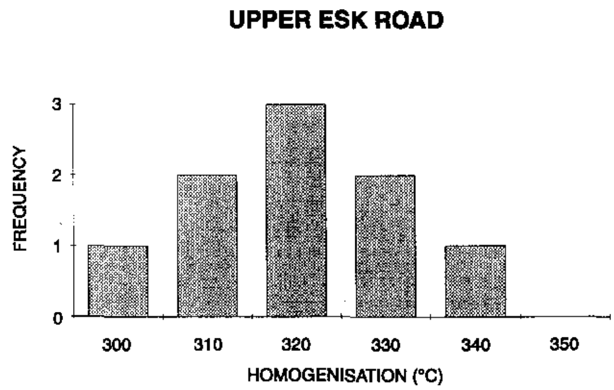

5 cm

Figure 9 (continued)

Only relatively early-formed primary-looking type B fluid inclusions were used for microthermometric measurements. The homogenisation temperatures from the Gorge Creek Tungsten prospect range from 224 to 269°C and those from the Rossarden–Mangana Road range from 172 to 245°C. A few measurements from inclusions in euhedral quartz in vugs (sample 107212) exhibit lower homogenisation temperatures being in a narrow range of 139.5 to 145°C. All of the inclusions homogenised to liquid.

Fluid Inclusion Composition-Freezing Experiments

The results from freezing experiments for type A2 and A3 fluid inclusions are very similar for most of the gold prospects from Mangana to Forester goldfields (Appendix 3).

Salinity measurements using the ice melting method are inaccurate in CO_2-bearing inclusions (type A2 and A3) due to clathrate formation (Poty *et al.*, 1974; Hollister and Burruss, 1976; Collins, 1981). However, the CO_2 hydrate melting temperatures may be utilised for salinity measurements provided no other gas species (e.g. CH_4) are present (Hollister and Burruss, 1976). This assumption may not be valid for this study, as the presence of CH_4 is indicated by the depressed final melting temperatures of CO_2 being in the range of -63 to -56.9°C (Burruss, 1981). The clathrate melting temperatures of fluid inclusions for A2 and A3 inclusions range from 8.8 to 12.5°C, above and below the invariant point of a pure CO_2 clathrate (Hollister and Burruss, 1976). Clathrate melting points of above 10°C suggest the presence of CH_4 in the fluid (Unruh and Katz, 1949; Hollister and Burruss, 1976). In general, it may be said that the high clathrate melting temperatures for type A2 and A3 fluid inclusions are consistent with a CH_4-bearing low salinity fluid.

The fluid inclusions from the Rossarden–Mangana Road area are very low in salinity, with the freezing points ranging from -0.4 to -0.8°C, whereas those from the euhedral quartz have lower freezing points, being in the range of -2.3 to -2.5°C, consistent with higher salinity fluids. A few fluid inclusions from the Gorge Creek Tungsten prospect were cooled below -100°C, but the size or shape of liquid and the vapour remained unchanged during the cooling.

Discussion

Despite the reconnaissance nature of this study, the results obtained from the fluid inclusion petrography and the microthermometric measurements appear to be significant in understanding the nature and the evolution of the mineralising hydrothermal fluid.

The close association of the different types of the CO_2-bearing fluid inclusions in quartz from most of the deposits (e.g. mines from the Mangana goldfield, Crown Prince mine) and their behaviour on heating and freezing may be explained by fluid immiscibility in the CO_2-H_2O system for the following reasons:

(a) the variability of the vapour to liquid ratios of inclusions within a single grain (i.e. CO_2-rich and H_2O-rich fluids);

(b) homogenisation of the inclusions to either vapour and liquid and occasional critical behaviour;

(c) no evidence of necking down or leakage.

No pressure correction is required to convert homogenisation to true formation temperatures if the fluid inclusions exhibit fluid immiscibility relationship, as both fluids are saturated with respect to each other. Assuming only a CO_2-H_2O system, a temperature range of 276 to 355°C is suggested for the main stage of gold and base metal mineralisation for the Mangana Gold Reef, West Miami, Argyle, and probably for the Strickland mines. However a similar fluid immiscibility relationship was not observed in fluid inclusions from the Linton and O'Brien mines, and therefore for these mines the homogenisation temperatures only indicate minimum formation temperatures. More systematic work is required to, firstly, establish statistically more reliable data and, secondly, to determine the importance of the boiling phenomenon in different goldfields.

Considering the critical temperatures for the CO_2-H_2O (297–328°C), then a pressure range of 400 to 550 bars is estimated for the main mineralising stage, using the experimental work of Takenouchi and Kennedy (1964). The CO_2 content of the fluid showing a critical phenomena ranges from 18 to 23 mole%.

Fluid immiscibility has been suggested in many metamorphic gold belts (e.g. Golfarb *et al.*, 1988; Craw, 1988; Ettner *et al.*, 1993) and other geological environments and is considered to have been the main control on deposition of many ore deposits (e.g. Eastoe, 1978; Spooner, 1980; Seccombe, 1990). Fluid inclusion results from the CO_2-bearing fluid inclusions support our field observations where hydrothermal brecciation of different generations was found to be common in most of the gold prospects visited. The occurrence of hydrothermal breccias suggests that the fluids exceeded the lithostatic pressure at different times, causing the fracturing and brecciation of the overlying rocks. A sudden drop in pressure (i.e. lithostatic to hydrostatic), due to either fracturing initiated by the above mechanism or movements along a pre-existing fault or shear zone, caused boiling, resulting in the exsolution of a CO_2-rich vapour. However the CO_2 content of the fluid appears to have been depleted in the last stages of white quartz deposition, and the fluid eventually became free of a CO_2 phase in euhedral quartz crystals grown in vugs (i.e. last stage of white quartz formation, sample 107212). This is indicative of the phase separation of the fluid during boiling; the CO_2 escaped from the system, having reacted with the country rocks and resulting in the fluid becoming increasingly depleted in CO_2 as the temperature dropped.

Bisulphide complexes (e.g. $Au(HS^-_2)$, $HAu(HS)^0_2$) are the most important gold complexes under low salinity, reducing conditions (Ahrland *et al.*, 1958; Pearson, 1973), and boiling is a very effective mechanism in deposition of gold from bisulphide complexes by decreasing the temperature and the activity of sulphide ligands in the fluid.

The low salinity, CO_2-H_2O (-CH_4) fluid inclusions and their narrow range in homogenisation temperatures along the northeast gold belt from the Mangana to Forester goldfields are indicative of typical metamorphic fluids. These metamorphic fluids appear to account for the formation of a very high proportion of the gold deposits within metamorphic and tectonic belts around the world occurring in different lithological successions and at different geological times (e.g. Fyfe *et al.* 1978; Fyfe and Kerrich, 1984; Neall and Phillips, 1987; Nwe and Grundmann, 1990; Golfarb *et al.*, 1988; Phillips and Powell, 1993; Ettner *et al.*, 1993). The similarity in fluid composition and in hydrothermal alteration and mineralisation, as well as oxygen isotope values (see oxygen isotope section) between different goldfields, are indicative of fluids with similar physical and chemical characteristics, and this in itself is reliable evidence that regional metamorphic fluids were most likely responsible for the formation of the main stages of the quartz veins and associated alteration and mineralisation within the area. However the exceptions are the fluid inclusions from the Gorge Creek Tungsten prospect (sample 107141), Rossarden–Mangana Road (107189), and from the quartz crystals in vug (sample 107212). Fluid inclusions from the Gorge Creek Tungsten prospect are distinctly different in that no CO_2 was detected upon freezing and they are lower in homogenisation temperatures. The salinity of these inclusions is not known at this stage of the study. The mineral assemblage for this prospect is also different from the other prospects along the belt in that it contains tourmaline, wolframite and generally is lower in gold grade (see *Geochemistry* and *Mineralogy* sections). This may be explained by the fact that the prospect is located within the contact metamorphic aureole of the Blue Tier Batholith. It is likely that granite-related fluids were responsible for the deposition of quartz veins and the associated mineralisation. This is also supported by the oxygen isotope results of quartz from this prospect, which are distinctly different from the oxygen isotope values of the quartz from the rest of the prospects along the gold belt (see later).

Fluid inclusions from sample 107189 show lower homogenisation temperatures than those measured from the Gorge Creek Tungsten prospect and are very low in salinity (~1 wt% equiv. NaCl). The results may indicate that a late, dominantly meteoric fluid was responsible for the formation of this quartz vein.

The fluid inclusions in euhedral quartz from vugs in different lodes probably represent the most modified (evolved) version of the original metamorphic fluid from which the early gold-bearing grey quartz was deposited, and it is inferred that its relatively low CO_2 content represents loss by boiling.

In summary, this study shows that:

(a) A H_2O-CO_2 rich fluid, probably metamorphic in origin, was responsible for the main stages of quartz veining and associated mineralisation.

(b) Boiling was probably the dominant mechanism responsible for gold precipitation, but other mechanisms such as fluid-wallrock interaction may have also contributed.

(c) In general the formation temperatures and the fluid compositions of the ore-forming fluids appear to be similar for the gold prospects along the belt from the Mangana to Forester goldfields.

(d) Euhedral quartz crystals in vugs in quartz lodes were probably formed from highly modified versions of the original metamorphic fluids.

(e) The different fluid compositions in quartz veins from the Gorge Creek Tungsten prospect are probably related to the intrusion of the nearby granite.

OXYGEN ISOTOPE STUDY OF QUARTZ LODES FROM MANGANA TO FORESTER GOLDFIELDS

Introduction

In general, elements used in stable isotope studies include C, H, O, S, B, and N, of which the isotope variations of carbon, oxygen, hydrogen, boron and sulphur are used in ore genesis studies. Some of the common features of these elements include low atomic mass, abundance in nature, and a relatively large mass difference between the abundant and rarer isotopes. The proportion of the rare isotopes (e.g. ^{34}S, ^{18}O) are still sufficient for accurate measurements by mass spectrometry.

Application of stable isotope geochemistry to the earth sciences was first described by Urey (1947). However the interpretations of data to ore genesis have been effectively used in the past 20 years (e.g. Ohmoto and Rye, 1979; Taylor, 1974, 1979; Ohmoto, 1986). Stable isotope data need to be interpreted in conjunction with other geological information such as structural setting, mineralogy, paragenesis, phase relationships, geochemistry and fluid inclusion studies. If this is done then useful information may be gained regarding the temperature of formation, source of carbon and sulphur, origins and redox states of ore-forming fluids, and evolution of hydrothermal fluids in ore deposits.

Oxygen and fluid inclusion studies have proven to be powerful techniques in studying the genesis of different mesothermal gold deposits (e.g. Rushton *et al.*, 1993; Ansdell and Kyser, 1992; Golfarb *et al.*, 1988; Ettner *et al.*, 1993; Böhlke and Kistler, 1986). This study was carried out to investigate the isotopic nature and origin of ore-forming fluids of some of the gold prospects along the belt.

The oxygen isotope analyses were carried out at the Geology Department, University of Tasmania. The reproducibility of the oxygen isotope analyses was within ± 0.2‰.

Oxygen Isotope Data

Twenty samples, consisting of the grey and white quartz veins from different mines and one quartz sample from a quartz sulphide pod in the Rex Hill granite, were analysed for oxygen isotopes (Table 7). The oxygen isotope results fall into three distinct categories:

1. High and consistent oxygen isotope values of different types of quartz from the West Miami, Golden Gate, Una, Linton, Golden Mara, Mangana Gold Reef, Mt Horror Gold, Long Struggle, Mercury, Strickland, Miner's Dream, and Crown Prince. These exhibit a narrow range of 16.0 to 17.7‰.

2. Oxygen isotope values from the Gorge Creek Tungsten prospect, which are lower than the above mentioned gold deposits, with a range of 13.4 to 14.5‰, and

3. The relatively light oxygen isotope value of a quartz sample (11.49‰) from a quartz sulphide pod in the Rex Hill granite.

The oxygen isotope compositions of water in equilibrium with the quartz at temperatures of formations determined by the fluid inclusion study, except for the Gorge Creek prospect, are shown in Table 7).

Discussion

The homogenisation temperatures obtained from the fluid inclusions from the Gorge Creek Tungsten prospect reflect the minimum formation temperatures (not corrected for pressure), and the oxygen isotope values of water were calculated at an assumed formation temperature of 300°C. This may also be true for a few other prospects where the immiscibility relationships were not observed (see fluid inclusions section). However, the overall conclusions should not be affected by assuming the same formation temperature of around 310°C for all the prospects showing CO_2-H_2O fluid inclusions at this level of investigation.

An average formation temperature of 350°C was assumed for sample 103994, using the fluid inclusion results of Groves *et al.* (1970) on some quartz-sulphide veins from the Rex Hill Granite. Assuming formation temperatures of 300°C for the quartz from the Gorge Creek Tungsten prospect and 350°C for the quartz sulphide pod in the Rex Hill Granite respectively, then water with a similar oxygen isotope values is indicated (Table 7). However, this needs to

Table 7

Oxygen isotope data, northeast Tasmania

Sample No.	Description	Location	^{18}O‰ SMOW	^{18}O‰ water	T (°C)
103994	quartz-sulphide pod	Rex Hill granite	11.91	6.6	350
003006	white quartz	Una	16.02	9.48	310
003006	grey mineralised quartz	Una	16.53	10.00	310
003003	white quartz	Strickland	16.52	9.98	310
003001	white quartz	Miners Dream	16.46	9.92	310
107141	mineralised white quartz	Gorge Creek Tungsten	13.4	6.88	300
107337	mineralised white quartz	Gorge Creek Tungsten	14.5	7.98	300
107176	grey quartz, laminated, diss sulphides	Mercury	16.9	10.36	310
107199	white quartz	West Miami	16.7	10.16	310
107207	white quartz	Mangana Gold	16.2	9.66	310
107251	laminate quartz, diss. sulphides	Long Struggle	17.7	10.16	310
107259	grey massive quartz	Golden Gate	16	9.46	310
107270	grey brecciated quartz	Una	17.2	9.66	310
107312	grey to white quartz	Linton	17.9	11.36	310
107330	white quartz	Mt Horror Gold	16.9	10.37	310
107335	banded grey quartz	Mt Horror Gold	16.9	10.37	310
107346	grey quartz	Golden Mara	16.7	10.16	310
107445	banded quartz	Pincher	16.00	9.46	310
107445	white quartz	Pincher	16.1	9.47	310

be confirmed by more detailed fluid inclusion and oxygen isotope studies.

The isotopically high and very consistent oxygen isotope values of quartz from the main stages of quartz veining, and the associated gold and minor base metal mineralisation, and also their similarities in formation temperatures and fluid compositions and the fact that these deposits are not anomalous in tin, tungsten or bismuth (see *Geochemistry* section), permit the following conclusions to be drawn:

1. The fluids responsible for the formation of the main stages of quartz veining and associated mineralisation have not been derived locally and represent typical CO_2-rich regional metamorphic fluids (e.g. Phillips and Powell, 1993; Ettner *et al.*, 1993; Craw, 1988; Ansdell and Kyser, 1992). The fluids were probably formed by devolatisation reactions during prograde metamorphism at depth.

2. Oxygen isotope values cannot be used as an exploration tool for the gold deposits formed mainly by metamorphic fluids because the early gold-bearing quartz and the later, mostly barren quartz, are isotopically identical. However the technique appears to be effective in differentiating the quartz lodes of metamorphic origin from those formed from other sources (i.e. granitic fluids).

Isotopically-lower oxygen isotope values from the Gorge Creek Tungsten prospect, in conjunction with the fluid inclusion microthermometry results, different mineral assemblages and elevated tin and tungsten values (see *Geochemistry* and *Mineralogy* sections) suggest that fluids responsible for the formation of this type of mineralised quartz vein have been derived from a different source. The similarity in the oxygen isotope compositions of water responsible for the formation of the quartz in the Gorge Creek Tungsten prospect with that in quartz-sulphide pod from the Rex Hill Granite suggests that the mineralised quartz veins at Gorge Creek were formed from magmatic dominated fluids exsolved from a crystallising granite. More oxygen isotope and fluid inclusion analyses of quartz are required to ascertain the involvement of other fluids (e.g. meteoric) and delineate any temperature zonation.

GEOCHEMISTRY

Introduction

The purpose of the geochemical study was to:

- investigate the relationships between gold and base metals in the gold deposits, to indicate potential pathfinder elements.
- differentiate and classify the gold-bearing quartz veins from the barren veins.
- investigate the potential for new forms of gold mineralisation e.g. disseminated and stockwork deposits.
- investigate the tin and tungsten contents of the samples for the different fields, and to establish whether these elements can differentiate between deposits of magmatic and metamorphic origin.

At this stage of this study, we have conducted about 270 gold analyses, plus 75 Cu, Pb, Zn, Ag, As; 109 Sn, Sb and W; and 19 Bi, Hg, Mo, Se and Te analyses (Appendix 2). Many more are in progress. Most samples are quartz veins of various types, some are host rocks.

The gold analyses were conducted within the department by fire assay-AAS finish (No. 103801–103827) and the remainder by AAS. This second method used 20 g of pulverised rock for aqua regia digestion prior to evaporation, MIBK extraction and analysis.

The base metals were analysed partly by XRF (No. 103801–103827), and the remainder by AAS, within the department. The other elements were analysed by XRF (No. 103801–103827 within the department, the remainder at AMDEL, Adelaide).

Results

The gold content of vein samples was related to the vein type as shown by the frequency distribution histograms in Figures 10, 11 and 12 and Table 8. These plots show that all quartz types can contain significant gold mineralisation, but some more than others. White (buck) quartz (without obvious grey quartz, lamination, brecciation, or sulphides) is usually unmineralised (in 70% of cases), but may contain up to 32 g/t Au and averages 1.0 g/t. Types of quartz other than white may be represented as several different categories on the graph, including grey, laminated, brecciated and sulphidic. Grey quartz usually contains more than 0.1 g/t Au, but ranges from <0.05 to >100 g/t, and averages 8.7 g/t; about 80% is mineralised. Laminated quartz rarely contains less than 0.1 g/t Au, usually contains more than 1 g/t Au, and sometimes contains more than 100 g/t, averaging 5.8 g/t. Brecciated quartz (containing slate clasts, etc.) usually contains more than 1 g/t Au, but ranges from <0.05 to 18 g/t and averages 2.3 g/t. Sulphidic quartz (with macroscopically visible sulphides, usually arsenopyrite or pyrite) usually contains more than 0.1 g/t Au, but ranges from <0.05 to 44 g/t, and averages 3.5 g/t. These results show that grey quartz is the most important gold host, followed by laminated and sulphidic quartz. Other styles are also important.

Host rocks (particularly mudstone) commonly contain gold (up to 0.6 g/t), although this may be related to micro-veining and more work is needed to define the nature of this mineralisation.

At this stage of the study there are insufficient data to correlate gold and most base metals, with the exceptions of As, W and Sb. The correlation of As and Au is shown in Figure 13. The correlation is positive but rather weak, with a correlation co-efficient of 0.071. Subdivision according to degree of weathering improves the correlation, probably indicating some remobilisation of As. Tin and W show no relationship to gold, and are only elevated in the Gorge Creek W and Mt Horror As prospects (fig. 14). The Au-W correlation co-efficient is 0.001. Sb shows a very weak relationship to gold, with a correlation co-efficient of 0.059, and is usually low in value (fig. 15). Anomalous Sn or W appears to be a reliable way of differentiating granite-related

Table 8

Distribution of gold values in different styles of quartz veins

Gold grade (g/t)	Vein style: grey	white	laminated	brecciated	sulphidic	non-white
<0.05	10	48	2	6	4	19
0.05–0.1	4	6	0	2	4	8
0.1–1	28	8	11	15	14	48
1–10	21	8	13	7	11	37
10–100	10	3	5	2	4	14
100–1000	2	0	1	0	0	2
Total	75	73	32	32	37	128

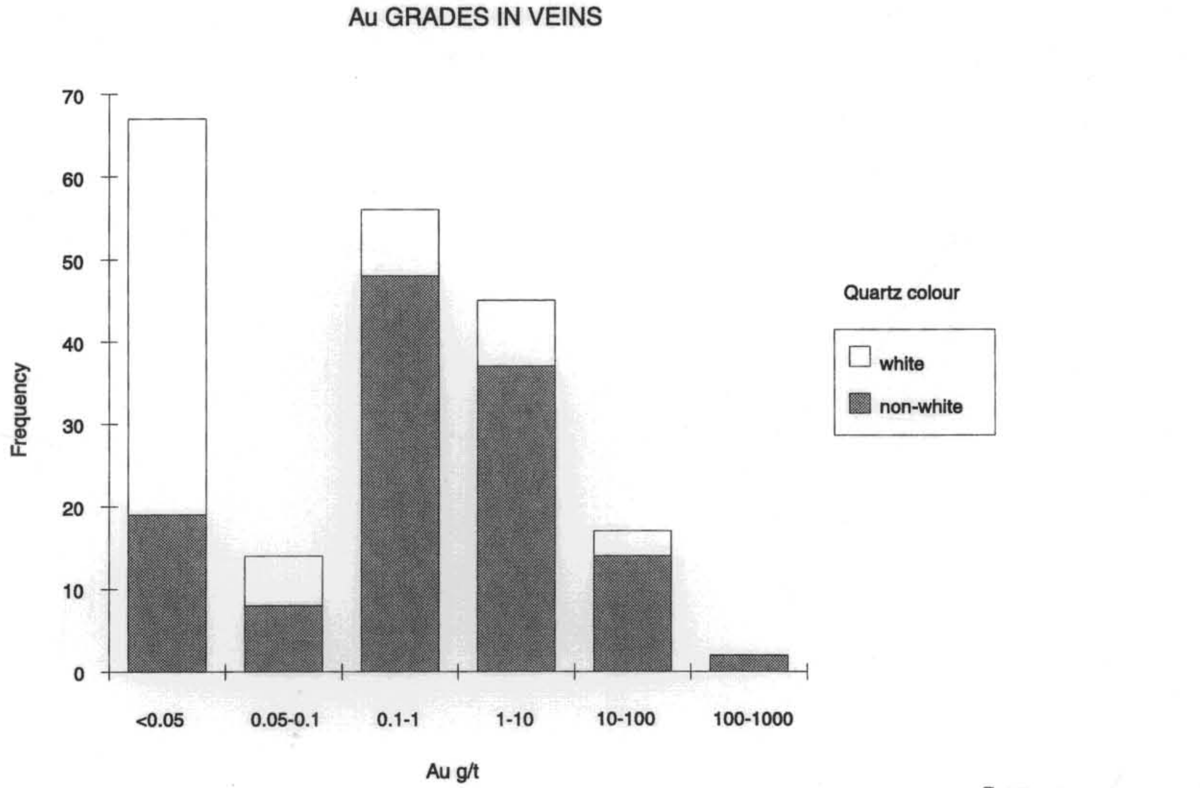

Figure 10

Gold content in buck quartz relative to other vein types

mineralisation. Gold may also show weak correlations with base metals. This requires further investigation, but probably indicates that gold was commonly deposited at the same time as sulphides, perhaps with a drop in sulphur activity, but the relationship was modified by later remobilisation.

GENESIS OF LODE-GOLD DEPOSITS OF THE MANGANA–FORESTER GOLD BELT

Discussion

Fluid inclusion and stable isotope studies, mainly of oxygen and hydrogen, have been effectively used in investigating the origin and the evolution of ore-forming fluids in shear zone-hosted veins within different tectonic belts. It has been shown that the fluids evolve during upward movement (Craw, 1990; Nwe and Grundmann, 1990 Rushton *et al.*, 1993) due to fluid-wall rock interaction, phase separation, boiling, and change in pressure and temperature . Therefore, we have tried to use our field observations, fluid inclusion, geochemical, isotopic and petrographical data to interpret the origin of the mineralising fluids and possible mechanisms on gold precipitation in the region.

Ore-forming fluids for mesothermal gold deposits

High temperature, low salinity, CO_2-rich fluids are the main source of ore-forming solutions along shear zones within metamorphic and tectonic belts (Craw, 1988; Ansdell and Kyser, 1992; Phillips and Powell, 1993). Fluids responsible for the formation of Archean greenstone gold deposits in slate belts, also known as turbidite-hosted or

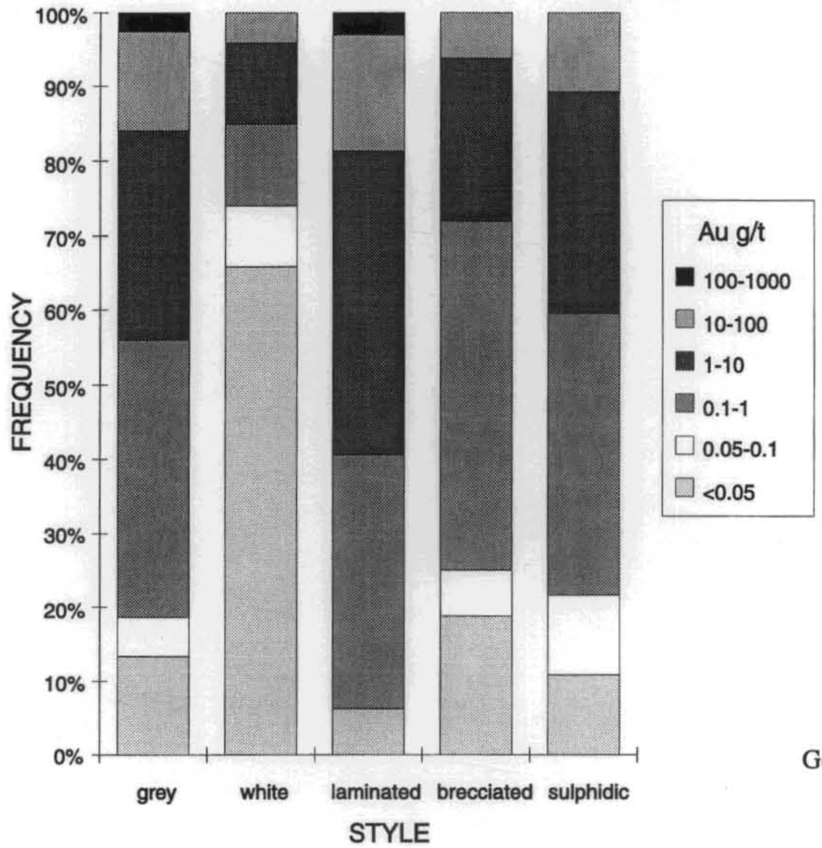

Figure 11

Gold distribution in various vein types

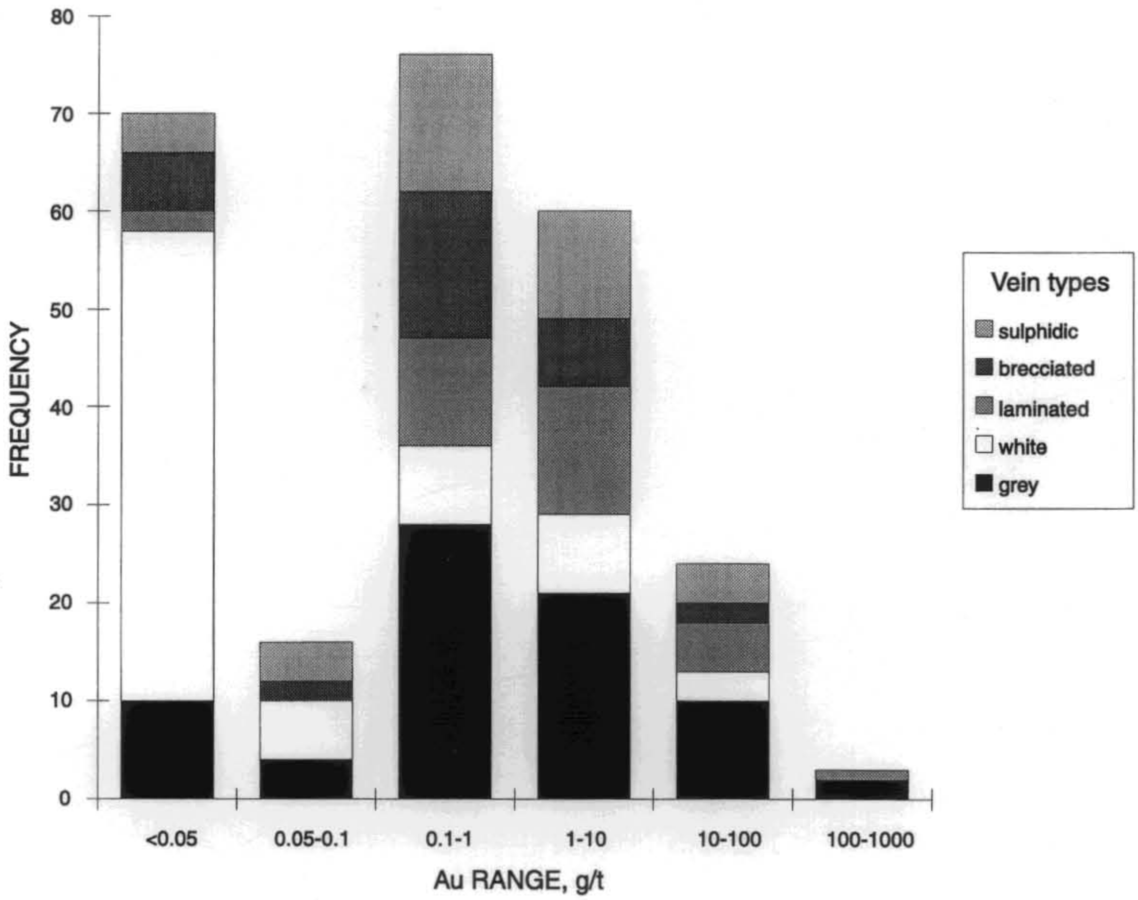

Figure 12

Distribution of various vein types relative to gold content

5 cm

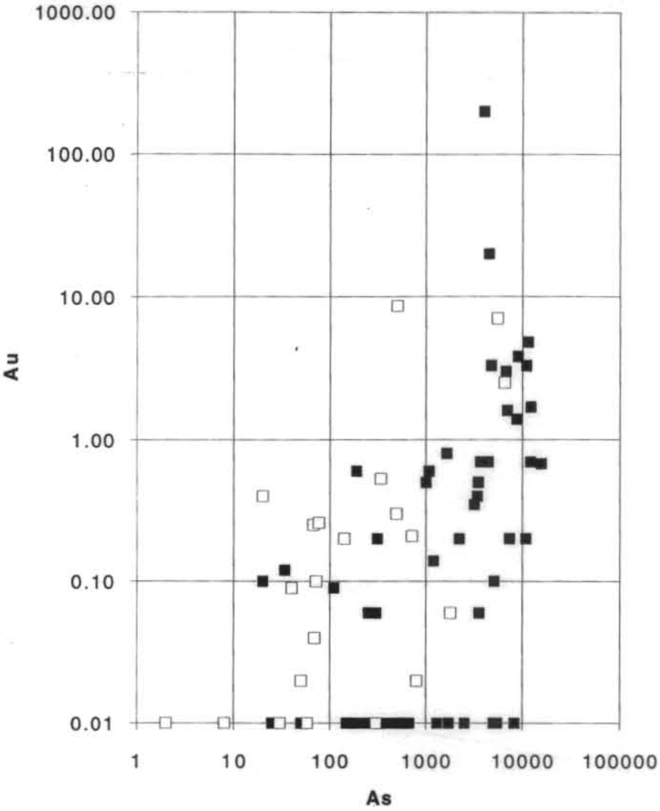

Figure 13

Plot of gold versus arsenic for various samples. ■ = unoxidised, □ = oxidised

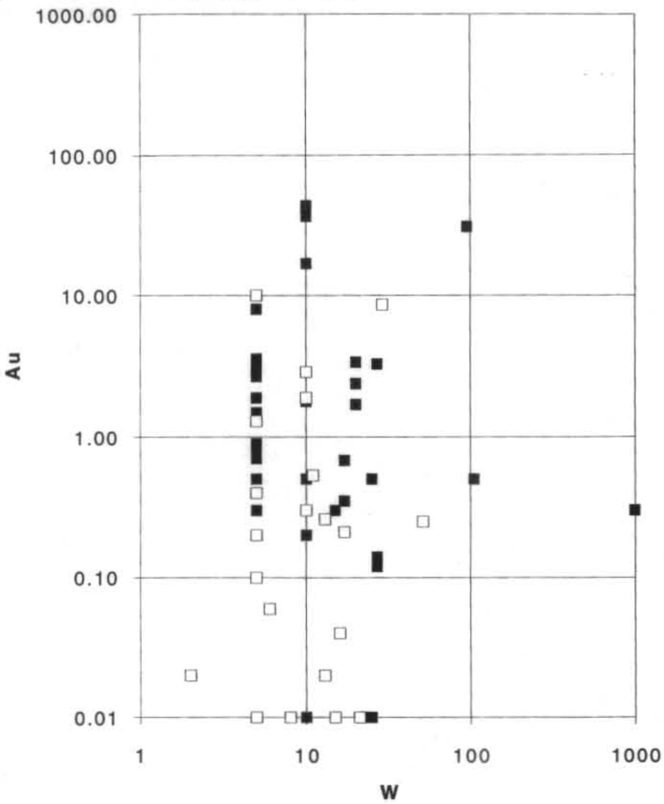

Figure 14

Plot of gold versus tungsten for various samples. ■ = unoxidised, □ = oxidised

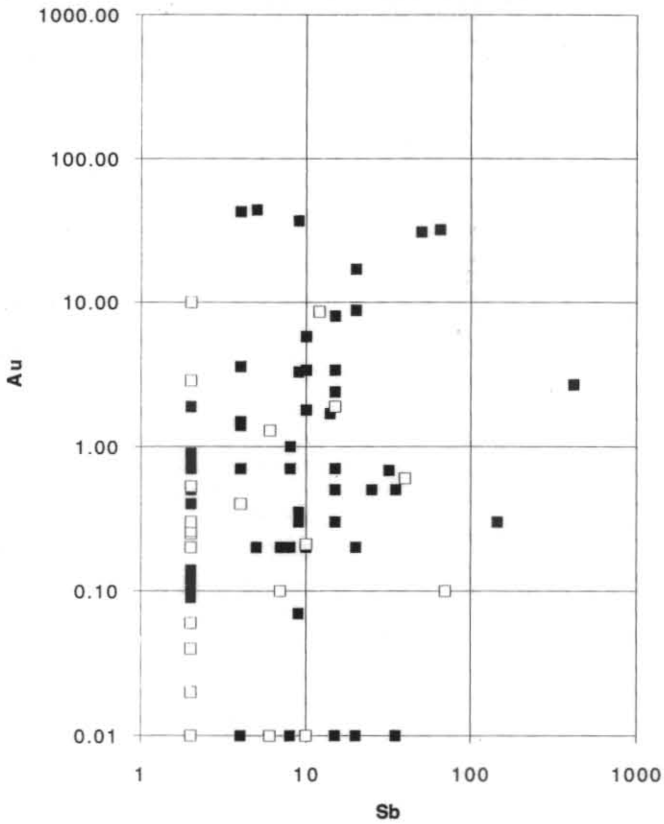

Figure 15

Plot of gold versus antimony for various samples. ■ = unoxidised, □ = oxidised

shale-greywacke gold provinces, have been studied in detail in some deposits (e.g. Ho *et al.*, 1990; Smith *et al.*, 1984; Groves and Phillips, 1987; Kontak *et al.*, 1990; Golfarb *et al.*, 1988).

A widely accepted origin for the CO_2-H_2O fluids responsible for the formation of mesothermal gold deposit is the generation of H_2O and CO_2 during prograde metamorphism under greenschist to amphibolite metamorphic facies conditions (e.g. Kerrich and Fyfe, 1981; Groves and Phillips, 1987; Phillips and Powell, 1993). According to Will *et al.*, (1990) the devolatisation of chlorite-calcite-albite-quartz (e.g. mafic-greywacke rocks) will produce large volumes of H_2O-CO_2 fluids at 4–5 kbars. Devolatisation of 1 km^3, involving the release of 1 mass percent of fluid from the original rocks, will produce over 10 million tonnes of fluid capable of transporting gold as reduced sulphur complexes (Phillips *et al.*, 1987). However, the metamorphic devolatisation model has been questioned by some workers (e.g. Shelton *et al.*, 1988; Nesbitt, 1990; Rushton *et al.*, 1993). In general, these workers have proposed that gold-lode mesothermal deposits have been formed from chemically evolved, deeply circulated meteoric waters. This model, based on hydrogen isotope values, assumes that the deuterium values should retain much of the original meteoric signature, mainly due to the presumed low water/rock ratios (Nesbitt and Muehlenbachs, 1989). The oxygen isotope values of fluid, however, reflect the re-equilibration with the isotopic compositions of the host rocks.

Theoretical modelling of Connolly and Thompson (1989) is also supportive of involvement of fluids other than those of metamorphic origin for the formation of mesothermal quartz veins. They suggested that much of the fluid generated by devolatisation at depth is probably consumed by retrograde hydration reactions in the shallower depths of dehydrated rocks, and that the formation of quartz lodes would have required more fluid than could have possibly formed by devolatisation processes.

Our results from fluid inclusion, oxygen isotope, geochemical and petrological studies support a deep-seated, compositionally uniform, CO_2-rich fluid of low salinity as being responsible for the formation of quartz lodes along the gold belt. This is similar to the situation in many other mesothermal gold provinces. However there is no definite evidence to support either metamorphic or deeply convecting, evolved meteoric water for the origin of the fluids.

Extreme care must be taken in deducing the origin of fluids responsible for the formation of mesothermal quartz gold lodes solely from hydrogen isotope data. The common practice is to analyse muscovite or to extract fluid from fluid inclusions for deuterium analyses. However, muscovite may be isotopically re-equilibrated with descending meteoric fluids and give strongly depleted deuterium values. Bulk fluid extraction from fluid inclusions can also be erroneous, as late-formed low temperature secondary inclusions of meteoric origin are far more abundant than primary fluid inclusions in most quartz samples. The fluids may be a combination of both metamorphic and deeply convecting meteoric water.

Gold Transport

The solubility and deposition of gold in hydrothermal solutions has been discussed by many workers including Ohmoto (1986), Seward (1973, 1984), Crerar *et al.* (1985), Wood *et al.* (1987), Huston and Large (1989), and Hayashi and Ohmoto (1991), from which a summary is given below.

Gold mainly occurs as aurous ions (Au^+) in solution (Seward, 1973). It has a tendency to form covalent bonds, is strongly polarisable, and is classified as 'soft acid' or b-type cation (Ahrland *et al.*, 1958). Therefore aurous ions make the most stable complexes with soft bases such as HS^- (Pearson, 1973). Weakly polarisable (hard) bases, such as Cl^-, will form less stable complexes. 'Hard bases' also appear to behave similarly in forming complexes with metal cations, whereas soft bases tend to discriminate between the metals, with Au^+ being a favourable ion (Neall and Phillips, 1987).

The dominant bisulphide complexes include $Au_2(HS)_2S^{2-}$ (at high pH), $Au(HS)^-_2$ (at mildly alkaline pH), and $HAu(HS)^0_2$ (at near neutral to low pH) (Seward, 1973, 1984; Hayashi and Ohmoto, 1991). At pH values of less than 5.3 at 250°C and less than 6.2 at 350°C, $HAu(HS)^0_2$ is the most stable gold complex (Hayashi and Ohmoto, 1991). It is therefore considered to be the major transporting agent for the deposits discussed herein.

Chloro complexes become insignificant in low-salinity hydrothermal solutions for most mesothermal gold deposits.

Gold Deposition

The results from the fluid inclusion study indicate fluid immiscibility and subsequent phase separation of the mineralising fluids. The change from lithostatic to hydrostatic pressure due to tectonic activity or high fluid pressure forced the fluid through the solvus in the H_2O-CO_2 ($NaCl$-CH_4) system and resulted in formation of separate H_2O-rich and CO_2-rich fluid phases. The common occurrence of hydrothermal breccias, most of which are of autonomous in nature, suggests that fluid pressures above lithostatic pressures locally caused the fracturing of the overlying rocks or reopening of the veins.

Fluid immiscibility also causes the partitioning of other components such as H_2S and Au. In general, a decrease in aH_2S can bring about gold deposition by the following reactions (Hayashi and Ohmoto, 1991):

$$2Au(HS)^-_2 + H_2 + 2H^+ = 2Au + 4H_2S$$

$$2HAu(HS)^0_2 + H_2 = 2Au + 4H_2S$$

The effect of increase in solubility of gold by boiling (i.e. increase in fO_2) may be less than the reduction of aH_2S by oxidation:

$$4Au(HS)^-_2 + 2H_2O + 4H^+ = Au^0 + 8H_2S + O_2$$

and the equation showing the precipitation of gold from $HAu(HS)^0_2$ is:

$$4HAu(HS)^0_2 + 2H_2O = Au0 + 8H_2S + O_2$$

where the solution loses H_2S during boiling and precipitates gold. However the competing effects on gold solubility during boiling of oxidation and H_2S loss makes confident prediction difficult (Hayashi and Ohmoto, 1991). However the concurrent precipitation of sulphides would also promote gold precipitation (see later).

Early gold-bearing grey quartz appears to have been formed by silicification in some mines (e.g. Una) and contains fine, microscopic to sub-microscopic dark inclusions including rutile derived from the country rocks. It commonly also contains minor to abundant disseminated fine grains of arsenopyrite and other sulphides, and is probably the most important quartz type in terms of gold content within the area (see *Geochemistry* and *Mineralogy* sections for details). The grey colour is probably due to the combined occurrence of fine inclusions of carbonaceous country rock and very fine-grained sulphides. Laminated quartz veins formed by the crack and seal mechanism also contain sulphides and are generally gold rich. The close association of gold with sulphides right through the gold belt indicates that the formation of sulphides effectively reduced the sulphur activity of the ore-forming fluid and caused the precipitation of gold by destabilisation of Au-complexes. The fluid became exhausted in sulphur and metals (i.e. sulphide formation) but continued to form barren (i.e. white) quartz veins. The occurrence of minor, coarse-grained patches of sulphides and rare gold grains in the white quartz veins might have resulted from the remobilisation of the metals during later phases of deformation.

The fine, cherty nature of grey quartz and fine-grained disseminated sulphides may be indicative of sudden drop in temperature in the hydrothermal fluid and consequent supersaturation of the fluid with respect to silica. Boiling is effective for this cooling and the decrease in temperature favours sulphide precipitation. This loss of sulphur from the fluid would promote gold formation.

Sulphidation of wallrock could be a significant factor in precipitating gold from the mineralising fluids (i.e. also reducing the activity of sulphur). However, there is no field evidence to support this mechanism. The only significant wallrock alteration is 'carbonate spotting' where the slate and sandstone in close proximity to the lodes are characterised by small (<1 mm to a few millimetres) rounded porphyroblasts of Mg-siderite (see *Mineralogy* section). The carbonate alteration was probably a result of reaction between the CO_2-rich fluid and the host rocks prior to, or at the time of, mineralisation. Our limited field observations in the southern part of the belt (Mangana–Mathinna area) suggest that the 'carbonate spotting' is almost always associated with gold-bearing, sulphidic lodes rather than the barren ones. This may suggest that the later white, barren quartz veins were formed from fluids which were formed after the phase separation (CO_2 effervescence) and consequently there was not sufficient CO_2 in the solution to react with the host rocks. If this is true, then 'carbonate spotting' may be used as an indicator for locating gold-bearing lodes in the area.

Another important factor in precipitating gold is the occurrence of favourable host rocks, mainly rich in ferrous iron or carbon content. Equations describing the processes are:

$$4Au(HS)^0_2 + C + 2H_2O + 4Au + 8H_2S + CO_2 \text{ and}$$

$$4HAu(HS)^0_2 + 4\text{"FeO"(in silicate)} + 2H_2O$$
$$= 4Au + 8H_2S + 2Fe_2O_3$$

An excellent example is the Fe-rich rocks in Kalgoorlie hosting the gold mineralisation (Travis *et al.*, 1971). Nearly all the gold in the Archean Witwatersrand deposits are closely associated with Fe-rich conglomerates and carbon seams (Pretorius, 1981). However, as mentioned by Phillips and Powell (1993), the correlation between the gold deposits and host rocks does not exist in some terrains. An example is the Palaeozoic gold-bearing slate belt of Victoria, where the gold is hosted both by Lower Ordovician metasediments and the Cambrian mafic metavolcanics and Devonian mafic dykes (Phillips, 1991); the term 'slate belt' is misleading in this regard. Dark grey to black slate and soft carbonaceous? rocks (e.g. at Argyle), as well as siliceous sandstone and quartzite (e.g. Mt Victoria mine) host the gold mineralisation in the northeast of Tasmania. However there is no known correlation between the size and gold grades of the deposits and their host rocks.

Phillips and Powell (1993) have discussed the requirements for the formation of large mesothermal gold deposits. They suggest that factors such as a high geothermal gradient, favourable host rocks, structural regime, focusing of fluids, thick metamorphic piles undergoing devolatisation, absence of substantial erosion, and an early volcano-sedimentary alteration are all important in the formation of large lode-gold deposits.

It is well documented that the gold mineralisation in northeast Tasmania is structurally controlled and that the structures along the mineralised lineament appear to have been initially developed as wrench faults with some later reactivations (Keele, 1994). There is no evidence to support a correlation between the grade or size of the gold deposits and their host rock types or stratigraphic position. However the association of carbonaceous rocks with the gold mineralisation has been mentioned by many workers, including Keele (1994), and was first suggested by Twelvetrees in 1904.

Based on our field observations, fluid focusing appears to be one of the most important factors in the formation of high grade gold mines. Quartz lodes of considerable thickness and continuity are present in some of the gold, fields (e.g. Mangana). However, the gold prospectors in the past were very selective in mining of the quartz lodes. Adits were driven along the strike of the lodes but, commonly, they only extensively stoped one or two particular sections of the lodes without showing any interest in other parts (e.g. Mangana Gold Reef). Our geochemical results indicate that the 'untouched' areas of the lodes observed in different goldfields are generally barren or are very low in gold content. This may suggest that the most favourable physico-chemical conditions for the deposition of gold must have occurred in only certain areas of a lode (e.g. Mangana Gold) or a field (Golden Gate). A likely mechanism could be the formation of hydrothermally-formed pipes, where the fluid pressure locally exceeded the lithostatic pressure and brought about the deposition of gold and sulphides with boiling and loss of CO_2. Alternatively, the fluids may have been highly concentrated (channelled) in certain areas (e.g. at the intersection of two quartz lodes) causing the thickening of the early-formed grey quartz veins. There is no good field evidence for the proposed formation of pipe type deposits along the lodes, apart from the shapes of the stoped areas which are generally cylindrical to conical, and a small piece of hydrothermal breccia consisting of quartz and slate clasts which was observed right at the edge of a stoped area in adit 5 in the Mangana Gold mine. The main evidence for the possible thickening of the auriferous grey or laminated quartz in places along the quartz lodes is our observation from a few mines (e.g. Argyle) where the laminated sulphidic quartz or grey quartz pinches out immediately next to the worked quartz lode sections. This suggests that the thicker sections of gold-bearing quartz have been mined out. The main problem is the complete removal of gold-rich sections in almost every lode by the early miners, leaving no or very little evidence behind. The vertical extension of gold-bearing quartz sections in most of the worked areas of mines is not known and may be investigated by a systematic diamond drilling for the lodes. Our observations and model suggest that there is every possibility of grey gold-rich quartz occurring down-dip in the lodes from the barren white quartz.

CONCLUSIONS

Based on our field observations, together with petrological, geochemical, oxygen isotope and fluid inclusion studies, the following conclusions may be drawn:

- The gold mineralisation is of mesothermal type and is typical of many other 'turbidite hosted' gold-lode deposits.
- Numerous styles of of quartz veining can be identified; however only a few of these are significantly mineralised.
- The grey colour of the early-formed quartz is due to microscopic and submicroscopic grains of arsenopyrite, rutile, and carbonaceous material.
- Gold is commonly associated with stylolitic lamellae in grey quartz and is usually intimately associated with arsenopyrite.
- Most of the gold is free and the gold content of pyrite and arsenopyrite is usually low and probably not of great economic significance.
- In a few areas (Gorge Creek Tungsten deposit) granitic fluids appear to have been involved in remobilising gold from the nearby quartz-gold lodes. However this style of mineralisation is comparatively insignificant.
- Low salinity, CO_2-H_2O-rich fluids were responsible for the formation of gold deposits, with the exception of those mentioned immediately above, which were formed (remobilised) by granitic intrusions. The fluids were probably formed by devolatisation of the original metamorphic rocks, however deeply convecting, chemically modified meteoric fluids may have also played an important role.
- Reduction in the activity of H_2S, together with a decrease in temperature caused by boiling of fluids, appear to be the most effective mechanisms in precipitating sulphides in the early quartz veins. The sudden temperature decrease promoted formation of fine-grained (cherty) grey quartz and the formation of sulphides, and promoted gold precipitation. The occurrence of minor gold and relatively coarser quartz and sulphide grains in some white quartz veins may represent the remobilisation of the early formed sulphides and gold. Late, low-temperature barren quartz veins were formed after the phase separation process was completed.
- Fluid focusing appears to one of the most important factors in the formation of high grade gold mines.
- Wallrock-fluid interaction was of relatively minor significance in the formation of gold deposits along the lineament.
- Early sulphide and gold-bearing quartz veins were formed episodically by opening and closing of the extensional veins due to cyclic fluid pressure fluctuations ranging from supralithostatic to hydrostatic along shear zones. This process also produced hydrothermal breccias of possibly several generations.
- There is no field evidence to indicate a correlation between the size or the gold grade of the deposits and their host rock types or stratigraphic position.
- Mineralogically, the lodes which have formed from metamorphic fluids are quite different from those that resulted from the intrusion of granite bodies.
- There seems to be no distinct spatial zonation in the formation temperature of quartz lodes in the field. However this needs to be investigated in more detail.
- 'Carbonate spotting' is the most pervasive style of wallrock alteration associated with the gold-bearing quartz veins and may be used as an exploration tool in locating auriferous lodes.
- Fluid inclusion studies, oxygen isotope, and Sn and W analyses of the quartz lodes may effectively be used as three different techniques in differentiating the quartz formed from granitic vs metamorphic fluids.

ACKNOWLEDGEMENTS

We would like to thank Janine Triffett and Jane Mackey for lapidary preparation, Les Hay for chemical analyses, Richie Woolley for XRD work, and Gerrit Kuipers for the isotope analyses. Bob Findlay accompanied us in the field and contributed to discussions. We would also like to thank our wives for their patience and support.

REFERENCES

AHRLAND, S.; CHATT, J.; DAVIES, N. R. 1958. The relative affinities of ligand atoms for acceptor molecules and ions. *Quarterly Review Chemical Society* 12:265–276.

ANSDELL, K. M.; KYSER, T. K. 1992. Mesothermal gold mineralization in a Proterozoic greenstone belt: Western Flin Flon domain, Saskatchewan, Canada. *Economic Geology* 87:1496–1524.

ANTWEILER, J. C.; CAMPBELL, W. L. 1977. Application of gold compositional analyses to mineral exploration in the United States. *Journal of Geochemical Exploration* 8:17–29.

BLAKE, F. 1933. Preliminary report on New River goldfield. *Unpublished Report Tasmania Department of Mines* 1933:104–114.

BLAKE, F. 1938. Boring at Long Struggle mine – Alberton. *Unpublished Report Tasmania Department of Mines* 1938:1–4.

BLAKE, F. 1939. Mangana Goldfield. *Unpublished Report Tasmania Department of Mines.* 1939:75–110.

BLENKINSOP, T. G. 1988. Definition of low-grade metamorphic zones using illite crystallinity. *Journal of Metamorphic Geology* 6:623–636.

BÖHLKE, J. K.; KISTLER, R. W. 1986. Rb-Sr, K-Ar, and stable isotope evidence for the ages and sources of fluid components of gold-bearing quartz veins in the northern Sierra Nevada foothills metamorphic belt, California. *Economic Geology* 81:296–322.

BOIRON, M. -C.; CATHELINEAU, M.; TRESCASES, J .-J. 1989. Conditions of gold-bearing arsenopyrite crystallization in the Villeranges basin, Marche-Combrailles shear zone, France: a mineralogical and fluid inclusion study. *Economic Geology* 84:1340–1362.

BOTTRILL, R. S. 1992. The Mangana goldfield and adjacent gold mining areas. *Unpublished Report Tasmania Department of Mines* 1992/29.

BURRUSS, R. C. 1981. Analysis of phase equilibria in C-O-H-S fluid inclusions, *in* HOLLISTER, L. S.; CRAWFORD, M. L. (ed.). *Fluid inclusions, applications to petrology. Short Course Handbook Mineralogical Association of Canada* 6:39–74.

CABRI, L. J.; CHRYSSOULIS, S. L.; DE VILLIERS, J. P. R.; LAFLAMME, J. H. G.; BUSECK, P. R. 1989. The nature of "invisible" gold in arsenopyrite. *Canadian Mineralogist* 27:353–362.

CATHELINEAU, M.; IZQUIERDO, G. 1988. Temperature- composition relationships of authigenic micaceous minerals in the Los Azufres geothermal system. *Contributions to Mineralogy and Petrology* 100:418–428.

CATHELINEAU, M.; NIEVA, D. 1985. A chlorite solid solution geothermometer; the Los Azufres (Mexico) geothermal system. *Contributions to Mineralogy and Petrology* 91:235–244.

COLLINS, P. L. F. 1981. The geology and genesis of the Cleveland tin deposit, western Tasmania: Fluid inclusion and stable isotope studies. *Economic Geology* 76:365–392.

CONNOLLY, J. A. D.; THOMPSON, A. B. 1989. Fluid enthalpy production during regional metamorphism. *Contributions to Mineralogy and Petrology* 102:347–366.

COOK, N. D. J.; CHRYSSOULIS, S. L. 1990. Concentrations of invisible gold in the common sulfides. *Canadian Mineralogist* 28:1–16.

COX, S. F.; ETHERIDGE, M. A. 1993. Crack-seal fibre growth mechanisms and their significance in the development of oriented layer silicate microstructures *Tectonophysics* 92:147–170.

CRAW, D. 1988. Shallow-level metamorphic fluids in a high uplift rate metamorphic belt; Alpine Schist, New Zealand. *Journal of Metamorphic Geology* 6:1–16.

CRAW, D. 1990. Regional fluid and metal mobility in the Dalradian metamorphic belt, southern Grampian Highlands, Scotland. *Mineralium Deposita* 25:281–288.

CRERAR, D. A.; WOOD, S. A.; BRANTLEY, S. L.; BOCARSLY, A. 1985. Chemical controls on solubility of ore-forming minerals in hydrothermal solutions. *Canadian Mineralogist* 23:333–352.

DOWLING, K.; MORRISON, G. W. 1989. Application of quartz textures to the classification of gold deposits using North Queensland examples, *in* KEAYS, R. R.; RAMSAY, W. R. H.; GROVES, D. I. (ed.). The geology of gold deposits; the perspective in 1988. *Economic Geology Monograph* 6:342–355.

EASTOE, C. J. 1978. A fluid inclusion study of the Panguna porphyry copper deposit, Bougainville, Papua New Guinea. *Economic Geology* 73:721–748.

ETTNER, D. C.; BJØRLYKKE, A.; ANDERSON, T. 1993. Fluid evolution and Au-Cu genesis along a shear zone: a regional fluid inclusion study of shear zone-hosted alteration and gold and copper mineralization in the Kautokeino greenstone belt, Finnmark, Norway. *Journal of Chemical Exploration* 49:233–267.

FINDLAY, R. H. 1993. Report on visit to Victoria, Long Struggle and Linton mines, and to White's Alluvial Workings, Mangana, 30 June –1 July 1993. *Report Mineral Resources Tasmania* 1993/19.

FINUCANE, K. J. 1935. Mathinna and Tower Hill Goldfields. *Bull. geol. Surv. Tasm.* 43.

FYFE, W. S.; PRICE, N. G.; THOMPSON, A. B. 1978. *Fluid in the earth's crust.* Elsevier : Amsterdam.

FYFE, W. S.; KERRICH, R. 1984. Gold: natural concentration processes, *in* FOSTER, R. P. *Gold 82: the geology, geochemistry and genesis of gold deposits.* 99–127. Balkema : Rotterdam.

GOLFARB, R. J. ; LEACH, D. L.; PICKTHORN, W. J.; PATERSON, C. J. 1988. Origin of lode-gold deposits of the Juneau gold belt, southeastern Alaska. *Geology* 16:440–443.

GOSCOMBE, B. D.; FINDLAY, R. H., 1989. Mega-kinking in the Mathinna Beds, northeast Tasmania. *Report Department of Mines Tasmania* 1989/42.

GREEN, G. R. 1990. Palaeozoic geology and mineral deposits of Tasmania, *in* HUGHES, F. E. (ed.). Geology and mineral deposits of Australia and Papua-New Guinea. *Monograph Serial Australasian Institute of Mining and Metallurgy* 14:1207–1223.

GROVES, D. I. 1972. The zoned mineral deposits of the Scamander – St Helens district. *Bulletin Geological Survey of Tasmania* 53.

GROVES, D. I.; PHILLIPS, G. N. 1987. The genesis and tectonic control on Archean gold deposits of the Western Australian shield – a metamorphic replacement model. *Ore Geology Reviews* 2:287–322.

GROVES, D. I. ; SOLOMON, M.; RAFTER, T. A. 1970. Sulfur isotope fractionation and fluid inclusion studies at the Rex Hill mine, Tasmania. *Economic Geology* 65:459–469.

HANNINGTON, M. D.; SCOTT, S. D. 1989. Sulfidation equilibria as guides to gold mineralization in volcanogenic massive sulfides: evidence from sulfide mineralogy and the composition of sphalerite. *Economic Geology* 84:1978–1995.

HAYASHI, K.; OHMOTO, H. 1991. Solubility of gold in NaCl- and H_2S-bearing aqueous solutions at 250–350°C. *Geochemica Cosmochimica Acta* 55:2111–2126.

HILLS, C. L. 1923. The Mount Victoria goldfield. *Unpublished Report Tasmania Department of Mines* 1923:35–66.

HO, S. E.; BENNETT, J. M.; CASSIDY, K. F.; HORNSKY, J. M. A.; MIKUKI, E. J.; SANG, J. H. 1990. Fluid inclusion studies. *Publication Geological Department & University Extension, University of Western Australia* 20:198-211.

HOLLISTER, L. S.; BURRUSS, R. C. 1976. Phase equilibria in fluid inclusions from the Khtada Lake metamorphic complex. *Geochemica Cosmochimica Acta* 40:163–175.

HUGHES, T. D. 1947. The Dan Rivulet Goldfield. *Unpublished Report Tasmania Department of Mines* 1947:87–124.

HUGHES, T. D. 1952*a*. The Alberton goldfield. *Unpublished Report Tasmania Department of Mines* 1952:50–54.

HUSTON, D. L.; LARGE, R. R. 1989. A chemical model for the concentration of gold in volcanogenic massive sulphide deposits. *Ore Geology Reviews* 4:171–200.

KEELE, R. A. 1994. Structure and veining in the Devonian-aged Mathinna–Alberton gold lineament, northeast Tasmania. *Report Mineral Resources Tasmania.* 1994/06.

KERRICH, R.; FYFE, W. S. 1981. The gold-carbonate association: Source of CO_2 and CO_2 fixation reactions in Archean lode deposits. *Chemical Geology* 33:265–294.

KISCH, H. J. 1991. Illite crystallinity: recommendations on sample preparation, X-ray diffraction settings and interlaboratory samples. *Journal of Metamorphic Geology* 9:665–670.

KLOMINSKY, J.; GROVES, D. I. 1970. The contrast in granitic rock types associated with tin and gold mineralization in Tasmania. *Proceedings Australasian Institute of Mining and Metallurgy* 234:71–77.

KONTAK, D. J.; SMITH, P. K.; KERRICH, R.; WILLIAMS, P. F. 1990. Integrated model for Meguma Group lode gold deposits, Nova Scotia, Canada. *Geology* 18:238–242.

KRUMM, S.; BUGGISCH, W. 1991. Sample preparation effects on illite crystallinity measurement: grain-size gradation and particle orientation. *Journal of Metamorphic Geology* 9:671–677.

LEAMAN, D. E.; RICHARDSON, R. G. 1992. A geophysical model of the major Tasmanian granitoids. *Report Department of Mines Tasmania* 1992/11.

MAO, S. H. 1991. Occurrence and distribution of invisible gold in a Carlin-type gold deposit in China. *American Mineralogist* 76:1964–1972.

MCCLENAGHAN, M. P. 1985. Granitoids of northeastern Tasmania. *BMR Journal of Australian Geology and Geophysics* 9:303–312.

MCONIE, A. 1983. *A review of the gold potential of North Eastern Tasmania.* Goldfields Exploration Ltd [TCR 90-3140].

MONTGOMERY, A. 1892. Report on the Mathinna Goldfield. *Report Secretary of Mines Tasmania. 1891–92:40–58.*

NEALL, F. B.; PHILLIPS, G. N. 1987. Fluid-wall rock interaction in an Archean hydrothermal gold deposit: A thermodynamic model for the Hunt mine, Kambalda. *Economic Geology* 82:1679–1694.

NESBITT, B. E. 1990. Phanerozoic gold deposits in tectonically active continental margins, *in* FOSTER, R. P. (ed). *Gold metallogeny and exploration.* 104–132. Blackie : Glasgow.

NESBITT, B. E.; MUEHLENBACHS, K. 1989. Geology, geochemistry and genesis of mesothermal lode gold deposits of the Canadian Cordillera: Evidence for ore formation from evolved meteoric water, *Economic Geology Monograph* 6:553–563.

NOLDART, A. J.; THREADER, V. M. 1965. Gold deposits of Tasmania, *in:* MCANDREW, J. (ed.). Geology of Australian ore deposits. *Proceedings 8th Commonwealth Mining and Metallurgical Congress* 1:518–521.

NWE, Y. Y.; GRUNDMANN, G. 1990. Evolution of metamorphic fluids in shear zones: The record from the emeralds of Habachtal, Tauern Window, Austria. *Lithos* 25:281–303.

NYE, P. B. 1933. Preliminary report. The Ringarooma United mine. *Unpublished Report Tasmania Department of Mines* 1933:157–158.

OHMOTO, H. 1986. Stable isotope geochemistry of ore deposits, *in* VALLEY, J. W.; TAYLOR, H. P. jr; O'NEILL, J. R. (ed.). Stable isotopes in high temperature geological processes. *Reviews in Mineralogy* 16:491–559.

OHMOTO, H.; RYE, R. O. 1979. Isotopes of sulfur and carbon, *in* BARNES, H. L. (ed.). *Geochemistry of hydrothermal ore deposits.* 509–567. Wiley : New York.

PEARSON, R. G. (ed.). 1973. *Hard and soft acids and bases.* Dowden, Hutchinson and Ross : Stroudsburg, Pennsylvania.

PETERS, S. G.; GOLDING, S. D.; DOWLING, K. 1990. Mélange- and sediment-hosted gold-bearing quartz veins, Hodgkinson gold field, Queensland, Australia. *Economic Geology* 85:312–327.

PHILLIPS, R. G. 1991. Gold deposits of Victoria: A major province within a Palaeozoic sedimentary succession, *in: World gold 91.* 237–245. Australasian Institute of Mining and Metallurgy : Melbourne.

PHILLIPS, G. N.; POWELL, R. 1993. Link between gold provinces. *Economic Geology* 88: 1084–1098.

PHILLIPS, G. N.; GROVES, D. I.; BROWN, I. J. 1987. Source requirements for the Golden Mile, Kalgoorlie: significance to the metamorphic replacement model for Archean gold deposits. *Canadian Journal of Earth Sciences* 24: 1643-1651.

POTY, B.; STALDER, H. A.; WEISBROD, A. M. 1974. Fluid inclusion studies in quartz from fissures of Western and Central Alps. *Schweizerische Mineralogischer und Petrographischer Mitteilungen* 54:717–752.

POWELL, C. McA. 1991. Structure of the Beaconsfield and Lefroy goldfields. *Report Department of Mines Tasmania* 1991/16.

POWELL, C. McA.; BAILLIE, P. W. 1992. The tectonic affinity of the Mathinna Group in the Lachlan Fold Belt. *Tectonophysics* 214:193–209.

POWELL, C. McA.; BAILLIE, P. W.; CONAGHAN, P. J.; TURNER, N. J. 1993. The mid-Palaeozoic turbiditic Mathinna Group, northeast Tasmania. *Australian Journal of Earth Science* 40:169–196.

PRETORIUS, D. A. 1981. Gold and uranium in quartz-pebble conglomerates. *Economic Geology* 75th Anniversary Volume:117–138.

REID, A. M. 1925. The properties of the Ringarooma Gold Mining Company, Alberton, Tasmania. *Unpublished Report Tasmania Department of Mines* 1925:119–129.

REYNOLD, J. 1990. *A short course in fluid inclusion study.* Geology Department, University of Tasmania : Hobart.

RICKARDS, R. B.;DAVIDSON, G. J.; BANKS, M. R. 1993. Silurian (Ludlow) graptolites from Golden Ridge, NE Tasmania. *Memoirs Association of Australian Palaeontologists* 15:125–135.

ROACH, M. J. 1992. Geology and geophysics of the Lisle–Golconda goldfield, northeast Tasmania. *Bulletin Geological Survey Tasmania* 70:189–206.

ROCK, N. M. S.; GROVES, D. I. 1988. Can lamprophyres resolve the genetic controversy over mesothermal gold deposits? *Geology* 16:538–541.

ROEDDER, E. 1984. Fluid inclusions. *Reviews in Mineralogy* 12.

ROMBERGER, S. B. 1986. Mechanisms of deposition of gold in low-temperature hydrothermal systems. *Journal of Geochemical Exploration* 25:237. [abstract]

RUSHTON, R. W.; NESBITT, B. E., MUEHLENBACHS, K. 1993. A fluid inclusion and stable isotope study of Au quartz veins in the Klondike District, Yukon Territory, Canada: A section through a mesothermal vein system. *Economic Geology* 88:647–678.

SCOTT, J. B. 1933. Notes on the boring campaign at the northern end of the Alberton field (New River). *Unpublished Report Tasmania Department of Mines* 1933:69–70.

SECCOMBE, P. K. 1990. Fluid inclusion and sulphur isotope evidence for syntectonic mineralisation at the Elura mine, southeastern Australia. *Mineralium Deposita* 25:304–312.

SEWARD, T. M. 1973. Thio complexes of gold and the transport of gold in hydrothermal ore deposits. *Geochimica Cosmochimica Acta* 37:379–399.

SEWARD, T. M. 1984. The transport and deposition of gold in hydrothermal systems, *in* FOSTER, R. P. *Gold 82: the geology, geochemistry and genesis of gold deposits.* 165–181. Balkema : Rotterdam.

SHELTON, K. L.; SO, C. -S.; CHANG, J .-S. 1988. Gold-rich mesothermal vein deposits of the Republic of Korea: Geochemical studies of the Jungwon gold area. *Economic Geology* 83: 1221–1237.

SMITH, T. J.; CLOKE, P. L.; KESLER, S. E. 1984. Geochemistry of fluid inclusions from the McIntyre–Hollinger gold deposit, Timmins, Ontario, Canada. *Economic Geology* 79:1265–1285.

SPOONER, E. T. C. 1980. Cu-pyrite mineralization and sea water convection in economic crust; the ophiolitic ore deposits of Cyprus, *in* STRANGWAY, D. W. (ed.). The continental crust and its mineral deposits. *Special Paper Geological Association of Canada* 20:685–704.

TAHERI, J. (comp.). 1992. Northeast goldfields: a summary of the Tower Hill, Mathinna and Dans Rivulet goldfields. *Report Tasmania Department of Mines* 1992/10.

TAKENOUCHI, S.; KENNEDY, G. C. 1964. The binary system H_2O-CO_2 at high temperatures and pressures. *American Journal of Science* 262:1055–1074.

TAYLOR, H. P. jr. 1974. The application of oxygen and hydrogen isotope studies to problems of hydrothermal alteration and ore deposition. *Economic Geology* 69:843–883.

TAYLOR, H. P. jr. 1979. Oxygen and hydrogen isotope relationships in hydrothermal mineral deposits, *in* BARNES, H. L. (ed.). *Geochemistry of hydrothermal ore deposits.* 236–277. John Wiley : New York.

TAYLOR, B. 1992. *Structural traverse across the Mathinna Group, NE Tasmania.* B.Sc. (hons) thesis, University of Tasmania : Hobart.

THREADER, V. M. 1967. *The geology of the Mangana – Waterhouse goldfields, with particular reference to structure and mineralisation.* M.Sc. thesis, University of Tasmania : Hobart.

THUREAU, G. 1883. Report on the recently discovered goldfield at Mount Victoria, Country of Dorset, Tasmania. *House of Assembly Paper Tasmania* 1883(50).

THUREAU, G. 1884. Report on the Mount Victoria, Dan Rivulet, Black Boy and Mangana gold fields, also remarks after the examination of the Tullochgorum prospecting area. *Parliamentary Paper Tasmania* 1885(61).

TRAVIS, G. A.; WOODALL, R.; BARTRAM, G. D. 1971. The geology of the Kalgoorlie goldfield. *Special Publication Geological Society of Australia* 3:175–190.

TURNER, N. J.; BLACK, L. P.; HIGGINS, N. C. 1986. The St Marys porphyrite and related dykes: A Devonian intra-caldera ignimbrite and its feeder. *Australian Journal of Earth Sciences* 33:201–218.

TURNER, N. J.; CALVER, C. R. 1987. Geological Atlas 1:50 000 series. Sheet 49 (8514N). St Marys. *Explanatory Report Geological Survey Tasmania.*

TURNER, W. S. 1972. *Progress report on mineral exploration in the Mathinna–Tower Hill Goldfield, EL 6/68 — N.E. Tasmania to 30 September 1972.* Geophoto Resources Consultants, Minerals Report 1972/16 [TCR 72-923].

TWELVETREES, W. H. 1900. Report on the north Mount Victoria goldfield. *Report Secretary for Mines Tasmania* 1899–1900:xvii–xxx.

TWELVETREES, W. H. 1904. *Report on the Mount Victoria goldfield.* Department of Mines, Tasmania.

TWELVETREES, W. H. 1907. The Mangana goldfield. *Bulletin Geological Survey of Tasmania* 1.

TWELVETREES, W. H. 1914. On some gold-mining properties at Mathinna. *Rep. geol. Surv. Tasm.* 5.

UNRUH, C. H.; KATZ, D. L. 1949. Gas hydrates of carbon-dioxide-methane mixture. *Journal of Petroleum Technology* 1:83–86.

UREY, H. C. 1947. The thermodynamic properties of isotopic substances. *Journal Chemical Society (London)* 1947:562–581.

WILL, T. M.; POWELL, R.; HOLLAND, T. J. B.; GUIRAUD, M. 1990. Calculated greenschist facies mineral equilibria in the system CaO–FeO–MgO–Al_2O_3–SiO_2–CO_2–H_2O. *Contributions to Mineralogy and Petrology* 104:353–368.

WILLIAMS, E.; MCCLENAGHAN, M. P.; COLLINS, P. L. F. 1989. Mid-Palaeozoic deformation, granitoids and ore deposits, *in* BURRETT, C. F.; MARTIN, E. L. (ed.). Geology and mineral resources of Tasmania. *Special Publication Geological Society of Australia* 15:238–292.

WOOD, S. A.; CRERAR, D. A.; BORCSIK, M. P. 1987. Solubility of the assemblage pyrite-pyrrhotite-magnetite- sphalerite-galena-gold-stibnite-bismuthinite-argentite-molybdenite in H_2O-NaCl-CO_2 solutions from 200° to 350°C. *Economic Geology* 82:1864–1887.

WU, X.; DELBOVE, F.; TOURAY, J. C. 1990. Conditions of formation of gold-bearing arsenopyrite: a comparison of synthetic crystals with samples from Le Châtelet gold deposit, Creuse, France. *Mineralium Deposita.* 25 (Suppl.):S8–S12.

[8 April 1994]

APPENDIX 1

Illite crystallinity results

Sample No.	Location	Measured Peak Width	Recalculated Peak Width	Comment
F7 Ab	Upper Esk	0.40	0.29	
F8 Ab	Upper Esk	0.43	0.31	
F9 Ab	Upper Esk	0.39	0.28	hornfelsed
F21 Ab	Walkers Rd.	0.37	0.27	
F22 Ab	Merry Ck	0.35	0.25	
F25 Ab	Upper Esk	0.37	0.27	Biotite hornfels
F26 Ab	Upper Esk	0.37	0.27	
F31 Ab	Sweets Ck	0.41	0.29	hornfelsed
F40 Ab	King Ridge	0.36	0.26	
F41 Ab	King Ridge	0.36	0.26	
F42 Ab	King Ridge	0.36	0.26	
F47 Ab	Dorset River	0.36	0.26	
F48 Ab	King Ridge	0.35	0.25	
F49 Ab	Cross Reef	0.37	0.27	fresh
F49 Ab	Cross Reef	0.39	0.28	weathered
F52 Ab	Upper Esk	0.35	0.25	micaceous sandstone
F59 Ab	Tyne River	0.36	0.26	
F65 Ab	Upper Esk	0.38	0.27	'micaceous sandstone, veined'
F66 Ab	Cokers Rd	0.36	0.26	
F68 Ab	City of Hobart	0.37	0.27	
F69 Ab	City of Hobart	0.37	0.27	
F70 Ab	City of Hobart	0.36	0.26	
F72 Ab	City of Hobart	0.37	0.27	
F73 Ab	City of Hobart	0.37	0.27	
F75 Ab	City of Hobart	0.36	0.26	
Au2	Eton Rd.	0.37	0.27	
Au5	Chinamens Corner	0.39	0.28	
Au6	Upper Esk	0.36	0.26	
Au7	Jimmy's Ck	0.37	0.27	
Au8	Jimmy's Ck	0.36	0.26	
Loc 460	Rayner Rd	0.37	0.27	
Loc 530	Golden Gate Rd	0.40	0.29	
Loc 535	Black Horse Gully	0.37	0.27	
104433	Golden Gate	0.36	0.26	'black, pyritic'
103890	Merry Ck	0.37	0.26	
103892	Griffen Rd	0.36	0.26	
103896	Eton Rd	0.37	0.27	kaolinised
103897	Eton Rd	0.36	0.26	kaolinised
107103	Mangana Gold Reef	0.37	0.27	purple
107104	Mangana Gold Reef	0.35	0.25	green
107106	Mangana Gold Reef	0.37	0.26	purple
107106	Mangana Gold Reef	0.35	0.25	green
107106	Mangana Gold Reef	0.35	0.25	olive
107108	Tower Hill Freehold	0.34	0.24	'black, spotted, magnetic'
107110	Strickland	0.37	0.27	quartz veined
107111	Strickland	0.38	0.27	sulphidic
107116	Crown Prince	0.37	0.26	'kaolinised, veined'
107124	Mt Victoria	0.35	0.25	green
107131	Mt Victoria	0.35	0.25	bleached
107132	Mt Victoria	0.35	0.25	kaolinised
107192	Miami	0.35	0.25	'green, siliceous'
107194	Miami	0.35	0.25	pyritic
107226	Argyle	0.37	0.26	'carbonaceous, pyritic'
107265	Strickland	0.38	0.27	quartz veined
107268	Una	0.39	0.28	quartz veined
107291	Linton	0.40	0.29	'yellow, kaolinised'

Sample No.	Location	Measured Peak Width	Recalculated Peak Width	Comment
107291	Linton	0.38	0.28	'grey, kaolinised'
107297	Linton	0.38	0.27	'kaolinised, black'
107300	Linton	0.35	0.25	'kaolinised, black'
107331	Mt Horror Au	0.35	0.25	hornfelsed
107333	Mt Horror Au	0.38	0.27	'hornfelsed, kaolinised'
107347	Golden Mara	0.40	0.29	grey
107351	Golden Mara	0.40	0.29	grey
107355	Golden Mara	0.40	0.29	sulphidic
107360	Painted Cliffs	0.38	0.27	'kaolinised, grey'
107363	S. Esk Br., Fingal	0.39	0.28	kaolinised
107380	Fingal Mine	0.35	0.25	'kaolinised, black, spotted'
107417	Golden Gate Rd	0.37	0.27	'kaolinised, grey'
107440	Majors Gully	0.37	0.27	'grey-brown, wthd'
107441	Majors Gully	0.35	0.25	black
107444	Blackboy Ridge	0.35	0.25	'green, pyritic'
107463	Specimen Hill	0.36	0.26	'kaolinised, purple'
107464	Specimen Hill	0.38	0.27	'kaolinised, green, spotted
107468a	Sunbeam	0.34	0.25	'green, spotted'
107468b	Sunbeam	0.36	0.26	green
107469	Sunbeam	0.34	0.24	green
107473	Mountaineer	0.35	0.25	'kaolinised, green, spotted'
107476	New Eldorado	0.34	0.25	'kaolinised, spotted'
107479	New Eldorado	0.36	0.26	'kaolinised, white'
107481	New Eldorado	0.36	0.26	'kaolinised, beige'

APPENDIX 2

Geochemical anlayses of samples

Reg. No.	I.D.	Au g/t	Ag g/t	Cu g/t	Pb g/t	Zn g/t	As g/t	Sb g/t	Bi g/t	W g/t	Hg	Mo	Se	Site	Type	Weathered
895029	103801	0.25	<5	49	<5	10	67	<5	<5	51	<5	13	<5	Tower Hill	Lode	Y
895030	103803	0.04	<5	5	13	<5	69	<5	<5	16	<5	9	<5	Majors Gully	Alluvium	Y
895031	103806	0.21	5	65	68	100	710	10	7	17	<5	11	<5	Golden Entrance	Breccia	Y
895032	103807	0.12	<5	25	12	32	34	<5	<5	27	<5	11	<5	Golden Entrance	Breccia	N
895033	103809	<0.02	<5	<5	7	17	<5	<5	<5	5	<5	6	<5	St Marys	Alluvium	Y
895034	103810	0.68	<5	5	11	14	15570	32	98	17	<5	7	<5	Crown Prince	Lode	N
895035	103811	3.3	6	13	195	27	4730	9	33	27	<5	10	<5	Ringarooma United	Grey & white	N
895036	103812	0.02	<5	<5	<5	8	800	<5	6	13	<5	5	<5	Mathinna Plains	Stockwork	Y
895037	103813	8.6	18	57	155	580	500	12	<5	29	6	<5	<5	Mathinna Plains	white; contam?	Y
895038	103814	<0.02	<5	5	10	6	8	<5	<5	21	<5	<5	<5	Mathinna Plains	Lode	Y
895039	103815	0.06	7	54	230	99	1790	<5	10	6	<5	7	<5	Revenue	Lode	Y
895040	103816	0.53	7	23	16	63	340	<5	<5	11	<5	7	<5	Revenue	Lode	Y
895041	103817	<0.02	5	7	8	19	58	<5	<5	8	<5	6	<5	Golden Horseshoe	Lode	Y
895042	103819	0.26	5	18	10	19	77	<5	<5	13	<5	5	<5	Golden Horseshoe	Lode	Y
895043	103821	0.02	34	<5	<5	5	50	<5	<5	<5	34	8	<5	Majors Gully	Limonite	Y
895044	103822	0.35	<5	<5	<5	27	3160	9	20	17	<5	8	<5	Crown Prince	Breccia	N
895045	103825	0.14	<5	<5	26	37	1200	<5	9	27	<5	11	<5	Ringarooma United	Lode	N
895046	103826	1.7	<5	<5	13	14	12160	14	78	20	<5	9	<5	Ringarooma United	Breccia, milky, sx	N
920417	103828	<0.2	<1				1300	<5		23				Golden Gate	Lode	N
920418	103829	<0.2	<1				300							Golden Gate	Lode	N
920419	103832	0.7	1				3700							Golden Gate	Lode	N
930765	103855 B	0.4	≤1	<50	<50	<20	3400		<100					Mt. Victoria	quartz	
930766	103857	2.5	<1	<50	≤50	<20	6500		<100					Mt. Victoria	grey-white, qtztc, apy	y
930767	103863	0.5	≤1	<50	250	70	3500		<100					Cross Reef	breccia	
930768	103866	1.4	1	<50	70	<20	8700		<100					Long Struggle	breccia	
930769	103868	0.2	≤1	<50	<50	30	310		<100					Mercury	vein	
930770	103869	4.8	1	<50	140	250	11400		<100					Mercury	breccia, milky + apy	
930771	103870	0.2	≤1	1600	<50	400	2200	<100	<100					Mercury		
930772	103871	3.3	≤1	<50	120	<20	11000	<100	<100					Mercury	breccia, milky + apy	
930773	103873	7	1	<50	<50	<20	5500	<100	<100					Forester #3	breccia, milky	y
930774	103874	0.1	<1	<50	<50	<20	<50	<100	<100					Forester #3	quartz	
930775	103875	0.4	≤1	<50	<50	<20	<50	<100	<100					Forester #2	mudstone	y
930776	103876	0.6	≤1	<50	80	<20	190	<100	<100					Forester #2	mudstone	
930777	103878	0.7	3	<50	560	≤20	12000	<100	<100					Forester #2	quartz	
930778	103879	3	4	<50	300	<20	6700	<100	<100					Forester #2	lamin., sx, grey/white	
930779	103880	20	60	<50	2300	490	4500	<100	<100					Forester #2	lamin., py, grey/white	
930780	103881	200	420	<50	1100	140	4000	<100	<100					Forester #2	lode	
930781	103882	0.2	≤1	<50	330	<20	7300	<100	<100					Forester #2	quartz	
930782	103883	0.7	3	<50	1900	<20	4400	<100	<100					Forester #1	lode	
930783	103884	0.1	2	<50	510	<20	5100	<100	<100					Forester #1	quartz	
930784	103886	0.1	2	80	190	140	72	<100	<100					Forester #1	limonite	y
930785	103888	<0.05	≤1	<50	<50	<20	<50	<100	<100					Forester #1	phyllite	
930786	103889	<0.05	2	<50	<50	<20	2500	<100	<100					Forester #1	slate	
930941	103891	<0.05	<1					<100						Merry Ck		y
930890	103893	<0.05					30	<100						Griffen		y
930891	103894	<0.05					300	<100						Golden Horseshoe		y
930942	103895	<0.05	S1					<100						Golden Horseshoe		y
930892	103898	0.2					140	<100						Miners Dream		y
930893	103899	0.09					40	<100						Miners Dream		y
920412	104432	<0.2	<1	<0.01	0.02	0.01	<100							Golden Gate	Lode	N
920413	104433	<0.2	<1	<0.01	0.02	0.01	<100							Golden Gate	Lode	N
920414	104434	<0.2	<1	<0.01	0.02	0.01	<100							Golden Gate	Lode	N
920415	104435	0.5	1.7	0.02	0.02	<0.01	1000							Golden Gate	Lode	N
920416	104436	<0.2	1.5	0.01	0.02	0.03	<100							Crown Prince	Basaltic dyke	N

Reg. No.	I.D.	Au g/t	Ag g/t	Cu g/t	Pb g/t	Zn g/t	As g/t	Sb g/t	Bi g/t	W g/t	Hg	Mo	Se	Site	Type	Weathered
930943	107102	<0.05												Tower Hill Road		y
930944	107105	<0.05												Mangana Gold Reef		
930945	107113	0.1												Strickland		
930894	107114	1.6					6950							Strickland	white	
930895	107115	0.2					10840							Crown Prince	pug	
930896	107118	<0.05					270							Una		
930946	107119	19												Una	breccia, grey, white	
930897	107121	0.09					110							Una		
930898	107122	0.8					1640							Una		
930899	107126	0.6					1080							Mt. Victoria	quartzite	
930900	107127	0.06					3580							Mt. Victoria		
930901	107128	<0.05					360							Mt. Victoria		
930902	107129	<0.05					150							Mt. Victoria		
930948	107130	<0.05												Mt. Victoria		
930949	107137	<0.05												Gorge Ck		y
930950	107140	<0.05												Gorge Ck		
930951	107141	2.2												Gorge Ck	massive, glassy	y
930952	107143	0.3												Gorge Ck		
930953	107144	0.3												Gorge Ck		
930954	107147	0.2												Ringarooma United		
930903	107148	<0.05					170							Ringarooma United		
930955	107149	<0.05												Ringarooma United		
930904	107155	<0.05					5460							Mt. Victoia		
930905	107156	0.06					300							Mt. Victoria		
909506	107157	<0.05												Mt. Victoria		
939507	107159	<0.05												Mt. Victoria		
930006	107160	0.06					250							Mt. Victoria		
930908	107161	<0.05												Mt. Victoria		
930907	107163	<0.05					1720							Mt. Victoria	quartzite	
930908	107164	<0.05					220							Mt. Victoria	quartzite	
930909	107165	<0.05					470							Mt. Victoria	quartzite	
930910	107166	<0.05					8260							Mt. Victoria	quartzite	
930959	107169	0.1												Mt. Victoria		
930911	107170	<0.05					4990							Mt. Victoria	quartzite	
930912	107171	3.8					9010							Mt. Victoria	milky + apy, qtzt	
930960	107172	S0.1												Mt. Victoria		
930913	107173	<0.05					280							Mt. Victoria	quartzite	
930961	107176	10												Mercury	laminated, grey/white, sx	
930914	107177	<0.05					670							Mercury		
930962	107178	0.1												Ringarooma United		
930915	107183	<0.05					530							Ringarooma United		
930963	107185	<0.05												Chinamens		y
930916	107186	0.3					490							OBriens		y
930964	107187	18												OBriens	brecciated, grey/white	
930997	107189	0.07												Rossarden Rd		y
930998	107190	<0.05						<4						Rossarden Rd		y
930999	107191	<0.05												Miami	white	
931000	107193	<0.05						4						Miami	white	
931001	107196	<0.05												Miami	white	
931002	107197	<0.05												Miami	white	
931003	107198	<0.05												Miami	white	
931004	107200	<0.05												Miami	lim+qtz	y
931051	107201	0.3												Mangana Gold Reef	Sx, grey, white, breccia	
931052	107202	<0.05						<4						Mangana Gold Reef	white	
931005	107205	<0.05												Mangana Gold Reef		y
931006	107206a	<0.05												Mangana Gold Reef	white	
931007	107208	0.08												Mangana Gold Reef	white, Sx	y
931008	107209	<0.05												Mangana Gold Reef	white	y
931009	107210	<0.05												Mangana Gold Reef	white	y
931010	107211	<0.05												Mangana Gold Reef	white	

Reg. No.	I.D.	Au g/t	Ag g/t	Cu g/t	Pb g/t	Zn g/t	As g/t	Sb g/t	Bi g/t	W g/t	Hg	Mo	Se	Site	Type	Weathered
931011	107212	<0.05						<4						Mangana Gold Reef	white	y
931012	107213a	<0.05												Mangana Gold Reef	white	
931013	107213b	0.1												Mangana Gold Reef	Sx, grey	
931014	107214	0.1												Mangana Gold Reef	white qtz, Mn	y
931015	107215	0.2												Mangana Gold Reef	white, lam., sx	
931053	107216	0.2												Sovereign	white, lam., sx	
931016	107217	<0.05												Sovereign	white	
931055	107219	<0.05												Sovereign	white	
931017	107222	<0.05						10						Argyle-lower	slate	
931018	107224	<0.05						35		25				Argyle-lower	white	
931019	107227	0.4												Argyle-lower		
931020	107228	<0.05						10						Argyle-lower	white	
931021	107229	<0.05												Argyle-lower	white	
931022	107230	<0.05												Argyle-lower	white	
931023	107231	0.06												Argyle-lower		
931024	107234	<0.05												Golden Entrance	white, vuggy	
931025	107235	0.09						<4						Golden Entrance		
931026	107236	0.3												Golden Entrance		y
931027	107237	<0.05						20		10				RinGolden United	white	
931028	107238	<0.05												RinGolden United	white	
931029	107240	<0.05						<4						RinGolden United	white	
931030	107246	0.2												Mt. Victoria	white, grey, apy	
931031	107247	<0.05						10		15				Mt. Victoria	white, sx	
931032	107250	0.2						8						Long Struggle		
931055	107251	43						4						Long Struggle	white, laminated, apy	
931033	107252.1	8.8						20						Long Struggle	grey/glassy, laminated	
931034	107252.2	0.5						25		10				Long Struggle	grey/glassy, lam., apy	
931035	107253	1.9												Mercury	grey/white, lam., co3	
931036	107254	3.4												Mercury	grey/white, laminated	
931056	107255	<0.05						15		10				Mercury	white, vuggy	
931037	107258.1	<0.05						<4						Golden Gate	white, vuggy, ank, breccia	
931038	107258.2	<0.05												Golden Gate	grey, white	
931039	107258.3	<0.05						<4						Golden Gate	white	
931040	107258.4	<0.05						<4						Golden Gate	grey, white	
931041	107259	0.4												Golden Gate	grey, white	
931042	107266	1.5												Strickland	white	
931043	107267	<0.05						<4						Strickland	white	
931044	107268	<0.05						<4						Una	breccia, grey, white	
931057	107270	9												Una	breccia, grey, white	
931045	107272	0.07						9						Una	breccia, white	
931046	107273.1	<0.05												Una	grey	
931047	107273.2	<0.05						4						Una	grey	
931058	107274	<0.05												South Mangana	white	y
931059	107276	<0.05												South Mangana	white	y
931060	107277	<0.05												South Mangana	white	y
931061	107278	0.05												Argyle-upper	white	
931062	107281	2.3												Argyle-upper	white	
931063	107284	<0.05												Argyle-upper	white	
931064	107285	<0.05						<4						Argyle-upper	white, grey	
931065	107286	<0.05												Argyle-upper	white, grey	
931048	107287	2.5												Argyle-upper	white, kaol.	
931049	107288	7.4												Argyle-upper	white, vuggy	
931050	107289	5.8						10						Argyle-upper	white & brown	
931080	107291	0.08												Linton	slate	
931081	107292	24												Linton	grey/white, laminated	
931082	107293	0.6						40						Linton		y
931083	107295	<0.05												Linton	slate	
931084	107298	0.1												Linton		
931085	107299	<0.05												Linton		
931089	107301	2.9						<4		10				Linton	white, sx, lim	y

Reg. No.	I.D.	Au g/t	Ag g/t	Cu g/t	Pb g/t	Zn g/t	As g/t	Sb g/t	Bi g/t	W g/t	Hg	Mo	Se	Site	Type	Weathered
931090	107302	1						8						Linton	grey	
931091	107305	109												Linton	grey/brown, laminated	
931092	107306	0.2												Linton		
931093	107308	6.9												Linton	grey/white, laminated	
931094	107314	1.1												Linton	grey/white, lam., apy	y
931095	107327	1.2												Linton	grey/white, laminated	y
931096	107330	4.3												Mt Horror Au	grey/white, laminated	y
931097	107332	1.8						10		10				Mt Horror Au	grey/white, mottled	
931098	107334a	100												Mt Horror Au	white?	
931099	107334b	17						20		10				Mt Horror Au	grey?, apy	
931100	107335	16												Mt Horror Au	grey/white, mottled	
931101	107337	0.5												Gorge Ck W	white, tur	
931102	107338	0.3						<4		990				Gorge Ck W	white, crystals	
931103	107339	0.1												Gorge Ck W	white, Tur, Cv?	
931104	107342	0.5						<4		105				Gorge Ck W	vuggy, white, +Wf, Py	
931105	107343	<0.05												Mt Horror As	gossany	y
931106	107344	<0.05						6		15				Mt Horror As	Sx?	y
931107	107346	44						5		10				G Mara	grey-white, slatey, py	
931108	107349	31						50		95				G Mara	laminated, blue	
931109	107350	0.3						145		15				G Mara	brecciated, slatey	
931110	107353	0.6												G Mara	white,grey, laminated	
931111	107354	0.3						<4		10				G Mara	vuggy, laminated	y
931112	107356	8						15		<10				G Mara	white,grey, laminated	
931113	107358	0.05												D Dream		y
931114	107359	0.2						<4		<10				S Lode	white	y
931115	107361	<0.05												P. Cliffs		y
931116	107365	<0.05												Fingal Bridge	white	y
931117	107366	<0.05												Pincher	white	
931118	107367	<0.05						<4		<10				Pincher	white	
931119	107369	14												Pincher	white, brown, laminated	
931120	107370	32						65						Pincher	white, micaceous	
931121	107371	0.1						<4		<10				Pincher	quartzite	
931122	107373	21												Pincher	white, brown, laminated	
931123	107377	0.5												Fingal	white,grey, laminated	
931124	107379	0.2						5		<10				Fingal	pods	
931125	107381	0.1												Fingal	breccia	
940002	107403	1.9						<4		<10				Golden Gate	white, fg, + apy	
940003	107404	0.5						35		25				Golden Gate	blue,white, lam, brecc	
940004	107405	0.2						5		10				Golden Gate	massive, pale grey	
940005	107406	≤.05						<4		<10				Golden Gate	milky+grey lam.	
940006	107408	0.7						4		<10				Golden Gate	white, grey + apy	
940007	107412	0.7						8		<10				Golden Gate	white, grey brecc,+ apy	
940008	107413a	<0.05						8		10				Golden Gate		
940009	107413b	<0.05						10		10				Golden Gate		
940010	107413c	0.1						<4		<10				Golden Gate		
940011	107415	0.1												Golden Gate	slate+apy+veins	
940012	107421	≤.05												Mangana Gold Reef	qtz+Mn	
940013	107422	0.4						<4		<10				Sovereign	grey, apy	
940014	107423	2.7						420		<10				Mangana Gold Reef	grey, white	
940015	107425	0.5						15		<10				Mangana Gold Reef	white, brecc	
940016	107430	0.2						7		10				Mangana Gold Reef	grey, white, brecc	
940017	107431	0.5						<4		<10				Mangana Gold Reef	grey, white, brecc	
940018	107432	0.2												Mangana Gold Reef	brecc, py	
940019	107433	0.2						10		<10				Argyle-lower	brecc, white	
940020	107434	0.3						15		<10				Argyle-lower	grey/white	
940021	107435	0.3						9		<10				Argyle-lower	grey, sulphidic	
940022	107435b	0.3												Argyle-upper	grey, sulphidic	
940023	107436	0.1						70		<10				Argyle-upper	fg	y
940024	107437	1.4						4		<10				Argyle-upper	grey	

Reg. No.	I.D.	Au g/t	Ag g/t	Cu g/t	Pb g/t	Zn g/t	As g/t	Sb g/t	Bi g/t	W g/t	Hg	Mo	Se	Site	Type	Weathered
940025	107438	1.9						15		10				Argyle-upper	brown	y
940026	107439	3.4						10		<10				Argyle-upper	fg, white	
940027	107445	37						9		10				Pincher	grey, white, py, ms, lam	
940028	107446a	0.8						<4		<10				Pincher	grey, lam, ms	
940029	107446b	0.2						<4		<10				Pincher	white	
940030	107447	10						<4		<10				Pincher	white, grey, ms	y
940031	107448	≤.05												Fingal	white, brec	
940032	107449a	<0.05						<4		<10				Fingal		
940033	107449b	0.9						<4		<10				Fingal	grey, white, lam	
940034	107451	0.7						<4		<10				Fingal	breccia	
940035	107454a	1.5						4		<10				Mercury		
940036	107454b	2.4						15		20				Mercury		
940037	107455	≤.05						10		<10				Mercury	grey, white, lam	
940038	107456	3.4						15		20				Mercury	grey, white, lam	
940039	107457	0.2						20		<10				Long Struggle	white, lam	
940040	107458	0.2												Long Struggle	grey, white, lam	
940041	107459a	2.1												Long Struggle	grey, lam	
940042	107459b	<0.05												Long Struggle		
940043	107465	0.4						4		<10				Tower Hill F'hold	bluish, qtztc	y
940044	107466	0.7						15		<10				Sunbeam	grey, white	
940045	107467	3.6						4		<10				Sunbeam	brecc, white, apy, py	
940046	107474	2.9						<4		<10				Mountaineer	grey, white, lam, fg	
940047	107475	0.1						7		<10				Mountaineer	qtz-lim breccia	y
940048	107477	1.3						6		<10				New Eldorado	qtz-lim breccia	y
940049	107483	<0.05						10		15				New Eldorado		y
940050	107484	0.3						<4		10				New Eldorado		y

Abbreviations:

ank:	ankerite
apy:	arsenopyrite
brec:	brecciated
co3:	carbonate
cv:	covellite
fg:	fine grained
kaol:	kaolinitic
lam:	laminated
lim:	limonitic
Mn:	manganese oxides
ms:	muscovite
py:	pyritic
Qtz:	quartz
qtzt:	quartzitic
sx:	sulphidic
tur:	tourmaline
wf:	wolframite

APPENDIX 3

Fluid inclusion data, Northeast Tasmania gold prospects

Sample No.	Location	Description	QP/DP	composition	Inclusion type A1	A2	A3	B	g/t Au
103810B			QP/DP	H_2O, CO_2	y	y	y		?
103891	Merry Ck Rd		QP	H_2O, CO_2	–	y	y		<0.05
107105	Mangana GoldReef	White quartz with vugs	QP/DP	H_2O, CO_2	–	y	y		<0.5
107113	Strickland	White barren quartz	QP/DP	H_2O, CO_2?	y	y	y		0.1
107130	Mt Victoria, Adit #4	White quartz	QP/DP	H_2O, CO_2?	?	?	?		<0.05
107137	Gorge Tungsten Ck	White quartz, vuggy with late-formed veins	QP/DP	H_2O	–	–	–	–	<0.05
107141	Gorge Tungsten Ck	White quartz	QP/DP	H20,CO_2?	–	–	–	Y	2.2
107144	Gorge Tungsten Ck	White quartz with a bleb of sulphides	QP	H_2O	–	–	–		0.3
107146	Ringarooma United mine	Quartz veinlets in quartz porphyry	QP	–	–	–	–		
107147	Ringarooma United mine	Quartz veinlets in quartz porphyry	QP/DP	–	–	–	–		0.2
107157	Mt Victoria, Adit#4	White-grey quartz	QP	H_2O	?	?	?		<0.05
107169	Mt Victoria, Adit#4	Breccia (slate clasts with quartz matrix	QP/DP	H20,CO_2?	?	?	?		0.1
107161	Mt Victoria, Adit#4	White quartz vein with vugsl	QP	H20,CO_2	?	?	y		<0.05
107172	Mt Victoria, Adit#4	Banded white and grey quartz	QP	H20,CO_2?	?	?	?		0.1
107176	Mercury No 2	Grey quartz, fine banding, diss. sulphides	QP	H20,CO_2?	?	?	?		10
107185	Ringarooma	White quartz replacing slate	QP	H_2O	–	–	–	y	<0.05
107109	Strickland	Quartzvein		H_2O, CO_2?	–	–	–		
103900	Miners Dream	White quartz, vuggy	QP	H_2O	?	?	?		
107187	O'Briens		QP/DP	H20,CO_2	y	y	y		18
107123	Linton		QP/DP	H_2O, CO_2	–	y	?		
107178	Ringarooma		QP/DP	H_2O	–	–	–	y	0.1
107119	Una	Grey quartz with later-formed white quartz	QP/DP	H_2O, CO_2?	–	–	–		19
107120	Una		QP	H_2O	–	–	–		
107189	Rossardan-Mangana Rd.		QP/DP	H_2O	–	–	–	y	–
107190	Rossarden-Mangana Rd.	Massive quartz	QP	H_2O	–	–	–	Y	<0.05
107191	W. Miami	white quartz, vuggy	QP/DP	H_2O, CO_2	y	y	y		
107193	W. Miami	white quartz, vuggy	QP	H_2O	–	–	–		<0.5
107199	W. Miami	White quartz, massive	QP	H_2O, CO_2	y	y	y		
107201	Mangana Gold Reef	Grey quartz with sulphides along fractures	QP	H_2O	–	–	–		0.3
107202	Mangana Gold Reef	Breccia(slate and clay clasts, quartz matrix)	QP	H_2O, CO_2	?	?	y		<0.05
107204	Mangana Gold Reef	White quartz	QP	H_2O, CO_2	?	?	y		
107207	Mangana Gold Reef	White quartz with vugs	QP/DP	H_2O, CO_2	y	y	y		
107208	Mangana Gold Reef	white quartz	QP	H_2O, CO_2	y	y	y		0.08
107213	Mangana Gold Reef	White quartz	QP/DP	H_2O	–	–	–		<0.05
107214	Mangana Gold Reef	White quartz with vugs		H_2O, CO_2	?	?	Y		0.1
107215	Mangana Gold Reef	White quartz	QP	H_2O	–	–	–		0.2
107216	Mangana Gold Reef	White quartz, sulphide blebs, vuggy	QP	H_2O	?	?	?		0.2
107228	Argyle#2	White quartz with vugs	QP/DP	H_2O, CO_2	y	?	y		<0.05
107229	Argyle#2	White (vuggy) and grey (diss. sulphides) quartz	QP	H_2O, CO_2	y	?	y		
107231-3	Argyle#2	Sugary banded quartz with vugs	QP/DP	H_2O, CO_2	?	?	y		
107239	Ringarooma	White quartz with sericite	QP	H_2O	–	–	–		
107241	Ringarooma	quartz vein at contact with quartz porphyry	QP	H_2O	–	–	–		
107242	Ringarooma	Quartz vein in silicified slate	QP	H_2O	–	?	–		
107246	Mt Victoria #4	White quartz with vugs	QP/DP	H_2O, CO_2?	?	?	?		0.2
107248	Mt Victoria #4	White-grey quartz	QP	H_2O, CO_2?	?	?	?		
107250	Long Struggle	Banded grtey-white quartz	QP/DP	H_2O, CO_2?	?	?	?		0.2
107251	Long Struggle	Banded grey quartz diss. arsenopyrite	QP/DP	H_2O, CO_2?	?	?	?		43
107252-1	Long Struggle	Banded quartz, sulphides along boundaries	QP/DP	H_2O, CO_2	?	?	y		8.8

Sample No.	Location	Description	QP/DP	Inclusion type composition	A1	A2	A3	B	g/t Au
107252-2	Long Struggle	White quartz, open space filling	QP/DP	H_2O, CO_2?	?	?	y		
107254	Mercury #1		QP/DP	?	?	?	?		3.4
107255	Mercury #1?	Quartz crystal in vug	QP/DP	H_2O, CO_2	?	?	y		<0.05
107256	Golden Gate	Grey quartz with later-formed white quartz	QP	H_2O, CO_2?	?	?	?		
107258-1	Golden Gate		QP	H_2O	–	–	–		<0.05
107258-2	Golden Gate	White quartz		H_2O	–	–	–		<0.05
107259	Golden Gate	Grey quartz with diss. sulphides	QP	H_2O, CO_2	?	?	y		0.4
107260	Golden Gate	Breccia, slate clasts in quartz matrix	QP	H_2O, CO_2	?	?	y		
107265	Strickland	Grey quartz	QP/DP	H_2O	–	–	–		
107266	Strickland	White quartz	QP	H_2O, CO_2?	?	?	?		1.5
107270	Una	Grey banded quartz, pyrite along boundaries	QP/DP	H_2O, CO_2?	?	?	?		9
107273	Mangana (ridge)	White quartz veins in slate	QP/DP	H_2O, CO_2?	?	?	?		<0.05
107275	Mangana (ridge)	White quartz	QP	H_2O, CO_2	?	?	y		
107283	Argyle #1	White quartz	QP	H_2O, CO_2	?	?	y		
107284	Argyle #1	White quartz		H_2O, CO_2?	?	?	y		<0.05
107287	Argyle #1	White quartz with vugs	QP	H_2O, CO_2	?	?	y		2.5
107270	Una	Grey quartz	QP	H_2O, CO_2?	?	?	?		9
107310	Linton	Breccia	QP	H_2O, CO_2?	?	?	?		
107312	Linton	Grey-white quartz	QP/DP	H_2O, CO_2?	?	?	?		
107313	Linton	Grey-white quartz	QP/DP	H_2O, CO_2?	?	?	?		
107316	Linton	Gray and white quartz with late quartz veinlets	QP/DP	H_2O, CO_2?	?	?	?		
107318	Linton	Grey Quartz	QP	H_2O, CO_2?	?	?	?		
107324	Linton	White Quartz	QP	H_2O, CO_2?	?	?	?		
107330	Mt Horror Au	White-grey quartz	QP/DP	H_2O, CO_2?	–	–	–		4.3
107334	Mt Horror Au	Breccia	QP	H_2O	–	–	–		
107335	Mt Horror Au	Banded grey quartz with later white quartz	QP	H_2O	–	–	–		100,17
107337a	Gorge Ck W	White quartz	QP/DP	H_2O	–	–	–	y	16
107337b	Gorge Ck W	White quartz with tourmaline needdles	QP/DP	H_2O,solid incl.	–	–	–	y	0.5
107338	Gorge Ck W	White quartz	QP/DP	H_2O	–	–	–	y	
107339	Gorge Ck W	White quartz	QP	H_2O	–	–	–	–	–
107340	Gorge Ck W	White quartz	QP	H_2O	–	–	–		0.1
107342	Gorge Ck W	White quartz	QP	H_2O	–	–	–		
107343	Mt Horror As	White quartz	QP	H_2O	–	–	–		0.5
107344	Mt Horror As		QP	H_2O	–	–	–		<0.05
107346	Golden Mara	Grey massive quartz	QP	H_2O	–	–	–		<0.05
107353	Golden Mara	white quartz in sericitised rock	QP	H_2O	–	–	–		44
107354	Golden Mara	White quartz	QP	H_2O	–	–	–		0.6
107365	Fingal Bridge	White quartz	QP	H_2O	–	–	–		0.30
107366	Pincher		QP	H_2O, CO_2	?	?	y		<0.05
107367	Pincher		QP	H_2O, CO_2	?	?	y		<0.05
107369	Pincher		QP	H_2O	–	–	–		<0.05
107370	Pincher		QP	H_2O	–	–	–		14
107378	Fingal	Two generations of white quartz veins	QP	H_2O	–	–	–		32
107381	Fingal	Two generations of quartz veins	QP	H_2O	–	–	–		
107404	Golden Gate		QP						0.1

Fluid Inclusion Data

Sample No.	Location	Fluid inclusion type	Thl	Thv	Tm	Te	$TmCO_2$	TmClath.	$ThCO_2$	$ThCO_2 + H_2O$
107113	Strickland	A1							19.4 L	
		A2					-59.5	8.5-9.0	-	309 L
							-	9.0-9.5	-	299L
							-	-	-	318 C.P.?
							-	-	-	317 ?
							-	-	-	318 C.P.?
							-59.4	-	-	308L
107141	Gorge Creek W	B	269							
							301L			
			240							
										224
										227
										259
										258
										286 min.
										238?
107123	Linton	A2?					-64	12-12.5	CH_4- bearing	320L
										325L
										328L
										325L
										329L
										330L
107187	O'Brien	A3					-58.2	8.4-9.0	21.4L	308L
							-59	8.4-9.0	21.6L	276L
									22.0L	284L
										280L
									16.5L	285L
										292L
										289L
										301L
	Rossarden–	B	171.7		0.8					
	Mangana		225.5							
	Road		218		0.5					
			198							
			205							
			216		-0.5					
			211		-0.9					
			221							
			223							
			214		-0.8					
			229							
			232		-0.5					
			238							
			245							
107191	West Miami	A2?								322C.P.
										328V
										315?
										304L
										320C.P.?
										300V
										300L
										352V
										355L
										325V
										297L
		A3					-57.5	9.4-9.6		300V
									19.5L	
									19.6L	
									18.5?	280L
107207	Mangana	A3					57.1	8.8-9.0	22.9L	
	Gold Reef						-57.1	8.8-9.0	22.8L	
							-57		22.9L	
							-57	8.6-9.00		
							-57.2	9.0-9.2	22.7L	
			A1						24.4L	
							-57.4		26L	
							-57.4		27.2	
							-57.3			
									26.2L	
			A1						20.1L	276L
									25.2L	
									23.4L	

Sample No.	Location	Fluid inclusion type	Thl	Thv	Tm	Te	$TmCO_2$	TmClath.	$ThCO_2$	$ThCO_2 + H_2O$
		A2							25.9L	342V
									17.7L	
		A3							25.3L	343V
									28.1L	
		A3								284L
										291V
		A2								289V
										298C.P.?
		A3							22.1	298V
									22.3	289L
		A3								297V
		A1					-56.9		25.6L	
		A3					-56.9	8.9-9.3		
		A1					-56.9		25.5L	
		A2								297L
		A3							21.6L	297V
		A2								297L
		A2								275L
		A3								298V
		A2?								291V
		A2?								292V
		A2?					-57.2	10.9		254L
		A1							23.4L	
		A3					-57.5			
		A1							25.4L	
		A2								286
107228	Argyle	A3							25.4L	286
							-57	8.8-9.2	25.8	
		A2?								305V
		A3							23.2L	
		A3							24L	
		A2					-58.4	9.7		276L
		A3					-58.4		19L	259L
							-58.2	9.5-10	20.6L	
		A2								279L
		A3							19.5L	277-280L
F37AB	Simpson	A2						9.5-10		
							-58.5	9.5-10		
							-58.3	9.5		321-325V
							-57.9			321-325V
							-57.9	9.5		321-325V
		A3					-57.5	8.8-9.3		decrepitated
							-57.6	8.8-9.3	24.9L	decrepitated
							-57.2		23.4	
		A2								289L
										297?
3009	Crown Prince									285L
										310V
										310L
										297L
		A3					-57.8		23.2L	
		A2								272L
										283L
										310L
										324V or C.P
										293L
										325C.P?
		A2						9.8		328V or C.P.
										321V
								9.0-9.3		
							-58.2		13.2L	
							-58.5		12.2L	300.5L
3001	Miner's Dream	A3								307V
		A2								321V
										305L
		A3						8.8		
		A2?								305V
										310L
										315L
										334V
										330V
	5 411 050 mN									324V
	561 400 mE									348V
										321L
										324L